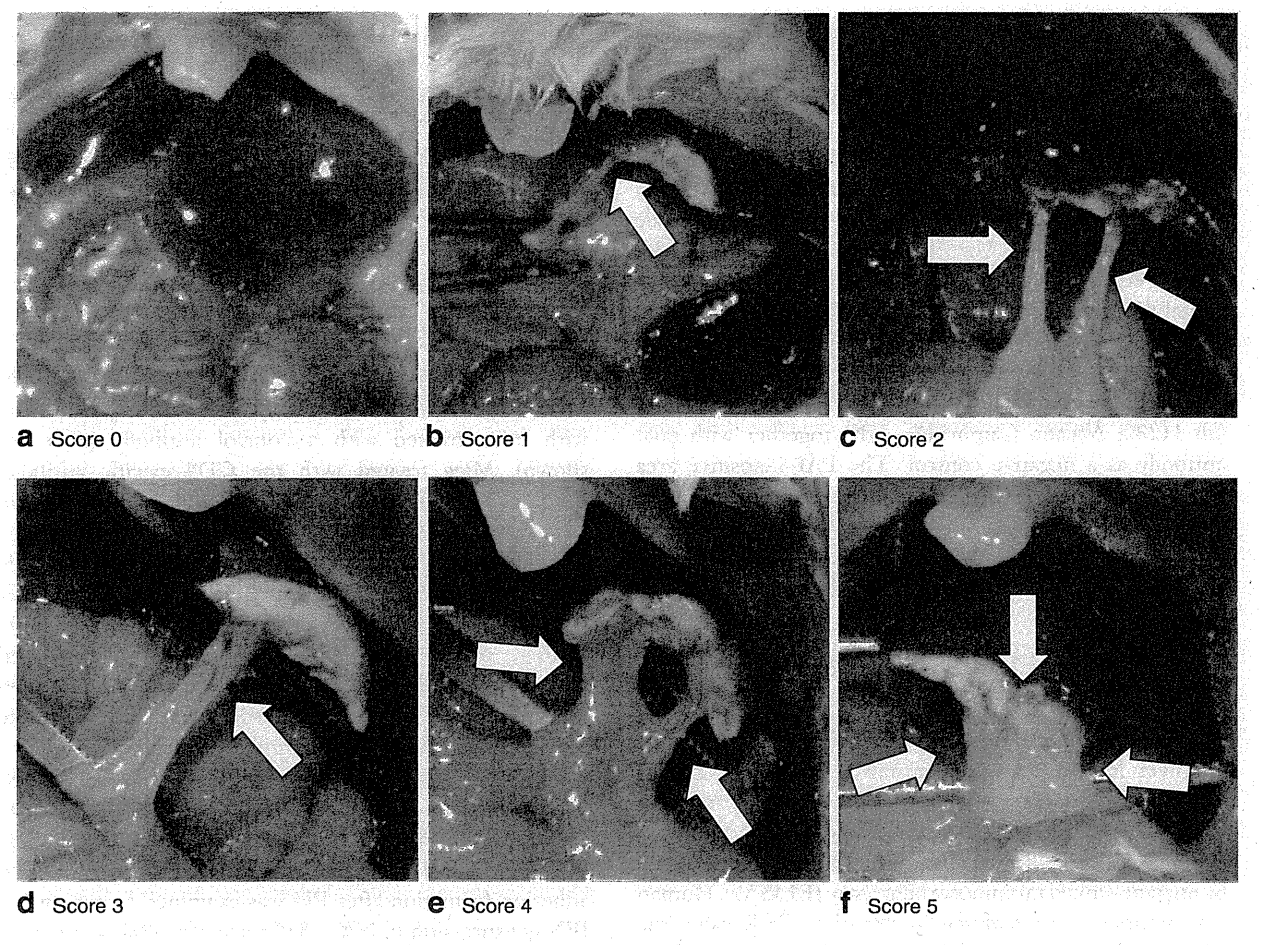

Fig. 1 Abdominal adhesion formation after partial hepatectomy (PH) in mice. Adhesions were evaluated according to a scoring system ranging from 0 to 5: **a** score 0, no adhesions (before PH); **b** score 1, a single thin filmy adhesion; **c** score 2, more than one thin adhesion; **d** score 3, thick adhesion with focal point; **e** score 4, thick adhesion with plantar attachment or more than one thick adhesion with focal point; and **f** score 5, very thick vascularized adhesion or more than one plantar adhesion. Arrows indicate adhesion sites. Typical images are shown from **a** BALB/c mice that had not undergone hepatectomy ($n = 2$), **b**,**c** interferon γ knockout mice 7 days after PH ($n = 5$) and **d**–**f** BALB/c mice 7 days after PH ($n = 12$)

Patients and liver specimens

All patients gave informed consent before surgery and the experiment was certified by the Ethics Review Board of Hyogo College of Medicine. Between January 2011 and January 2012, liver specimens were obtained from all patients who underwent a right- or left-sided hepatectomy at the Department of Surgery, Hyogo College of Medicine. Resection specimens were evaluated by a pathologist. Specimens with signs of liver cirrhosis were excluded. After laparotomy, the right or left hepatic artery and portal vein were clamped temporarily and the line of demarcation was identified on the surface of liver. Before parenchymal transection, about 1 cm^3 of liver tissue was harvested as a control specimen. Then, the resection line was marked along with the demarcation line. Liver biopsies of 1 cm^3 were obtained from the remnant liver before transection, and 1, 2 and 3 h after transection including the cauterized surface of the liver. The biopsies were analysed by haematoxylin and eosin staining, immunohistochemistry and quantitative reverse transcriptase (RT)–PCR.

Histology and immunohistochemistry

Liver biopsies from wild-type mice at all time points were stained with haematoxylin and eosin or Sirius red. Antifibrin antibody (A0080; Dako, Glostrup, Denmark)

was used to identify fibrin by immunostaining, as described previously[10].

Human liver biopsies were fixed in Zamboni solution for 2 days and frozen at −80°C. NKT cells were detected in frozen sections using an anti-NKT antibody (6B11; Miltenyi Biotec, Bergisch Gladbach, Germany) as well as 4,6-diamidine-2-phenylindole dihydrochloride (KPL, Gaithersburg, Maryland, USA) and a TSA™ kit (Life Technologies, Carlsbad, California, USA). Slides containing stained NKT cells were analysed by confocal microscopy (model 1X81; Olympus, Tokyo, Japan).

Immunohistochemical examination was carried out to detect expression of PAI-1 in human liver specimens (ab 31280; Abcam, Cambridge, UK) together with goat antibody as a negative control. The PAI-1-positive area in human liver samples was calculated using free software available from the National Institutes of Health (ImageJ; http://rsb.info.nih.gov/ij), on any five high-power fields (×100) from each of 11 human samples.

Quantitative RT–PCR and enzyme-linked immunosorbent assay

Total RNA was extracted from biopsies of the remnant left liver lobe of mice. Quantitative RT–PCR analysis was used to measure levels of IFN-γ, PAI-1 and tPA mRNA relative to the level of eukaryotic 18S rRNA as endogenous control[7]. PAI-1 protein levels were measured by enzyme-linked immunosorbent assay (ELISA)[7]. Human liver samples were analysed by real-time PCR using the same methodology. The human prehepatectomy liver samples were assigned a value of 1 as a control. The result for each liver sample after hepatectomy represents the fold change in mRNA compared with the control.

Statistical analysis

All continuous data are shown as mean(s.d.). Differences between two experimental groups were tested for significance with Student's *t* test. GraphPad Instat® Software (GraphPad, La Jolla, California, USA) was used. $P < 0{\cdot}050$ was considered significant.

Results

Intra-abdominal adhesions after hepatic resection in mice

The time course experiment revealed that PH induced progressive inflammatory and fibrotic changes, resulting in adhesions between the liver and bowel, greater omentum, pancreas or abdominal wall. Most wild-type mice formed thick adhesions with plantar attachment (score 4) or developed very thick vascularized adhesions (score 5) (*Fig. 1*). The histology of the liver at the site of injury is shown in *Fig. S1* (supporting information). Fibrin deposition in the liver after PH was already evident by 3 h following PH as well as after 1 day (*Fig. S2*, supporting information).

Natural killer T cell- and interferon γ-dependent adhesion formation in mice

$CD4^+$ T cells were depleted by more than 95 per cent in mice treated with the CD4-specific antibody compared with mice treated with a control antibody (data not shown). Mice treated with the CD4-specific antibody developed significantly fewer adhesions than control mice (adhesion score 1·0(0·3) *versus* 4·9(0·1) respectively; $P < 0{\cdot}001$) (*Fig. 2a*). Wild-type mice developed severe abdominal adhesions, whereas adhesions in NKT KO mice were of lower grade (adhesion score 4·6(0·4) *versus* 1·7(0·3) respectively; $P = 0{\cdot}037$) (*Fig. 2b*). Histological analysis revealed markedly reduced inflammation in NKT KO mice (*Fig. 2b*), indicating that NKT cells were indispensable for adhesion formation after PH.

Relative IFN-γ mRNA expression in the remnant left lobe of the liver peaked at 3 h after PH ($P = 0{\cdot}001$ *versus* before operation) and then decreased gradually (*Fig. 2c*). Whether IFN-γ released from NKT cells contributed to adhesion formation after PH was examined by measuring IFN-γ expression in NKT KO mice after PH; at 3 h after operation the level of IFN-γ mRNA was significantly reduced in the NKT KO mice compared with wild-type mice (*Fig. 2d*). In mice treated with IFN-γ-specific antibody and in IFN-γ KO mice, adhesion scores were reduced compared with those in control mice: 2·0(0) *versus* 4·4(0·6) ($P = 0{\cdot}020$) and 1·7(0·3) *versus* 4·4(0·6) ($P = 0{\cdot}002$) respectively (*Fig. 2e,f*).

Plasminogen activator inhibitor 1 regulated by interferon γ is key in adhesion formation

PAI-1 and tPA, which reciprocally regulate fibrin deposition, are known to act as primary regulators of the fibrinolytic system[11]. Remnant liver in wild-type mice showed increased levels of PAI-1 mRNA and decreased levels of tPA mRNA 6 and 18 h respectively after PH ($P = 0{\cdot}002$ and $P = 0{\cdot}026$ respectively) (*Fig. 3a,c*). The level of PAI-1 protein in plasma, measured by ELISA, was significantly increased at 3, 6 and 12 h after PH: 0·53(0·14) ng/ml ($P < 0{\cdot}001$), 0·82(0·31) ng/ml ($P = 0{\cdot}007$) and 0·81(0·22) ng/ml ($P = 0{\cdot}002$) (*Fig. 3b*).

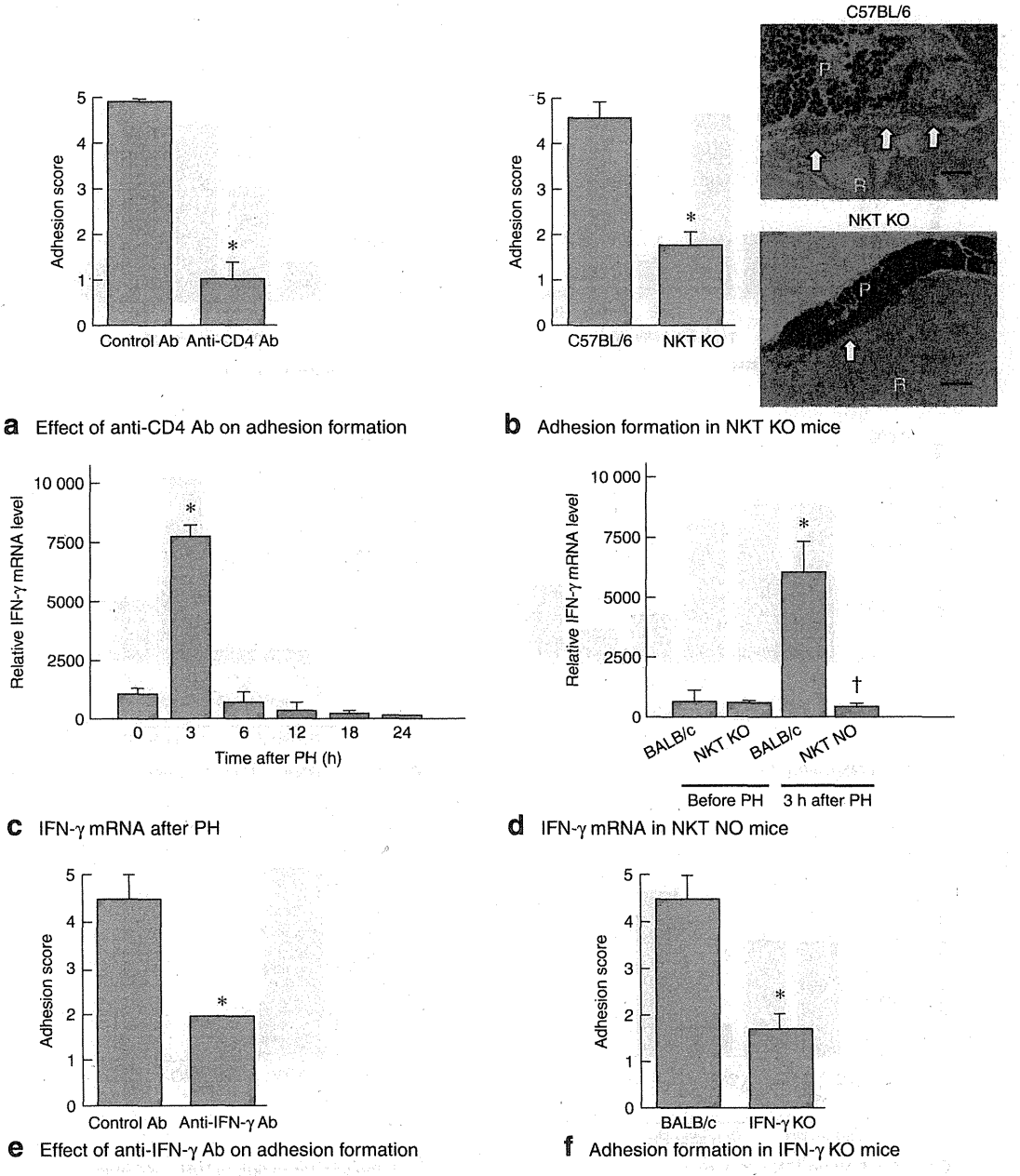

a Effect of anti-CD4 Ab on adhesion formation

b Adhesion formation in NKT KO mice

c IFN-γ mRNA after PH

d IFN-γ mRNA in NKT NO mice

e Effect of anti-IFN-γ Ab on adhesion formation

f Adhesion formation in IFN-γ KO mice

Fig. 2 Role of interferon (IFN) γ and natural killer T (NKT) cells in adhesion formation in mice examined 7 days after partial hepatectomy (PH). **a** Effect of depletion of $CD4^+$ T cells using anti-CD4 antibody (Ab) on development of adhesions. *$P < 0{\cdot}001$ *versus* control Ab. **b** Comparison of adhesion scores in wild-type (C57BL/6) and NKT knockout (KO) mice. *$P = 0{\cdot}037$ *versus* C57BL/6. Panels on the right show haematoxylin and eosin-stained sections, with weak inflammation in NKT KO mice. Arrows indicate sites of adhesion. R, remnant liver; P, pancreas (scale bar 200 μm). **c** Relative IFN-γ mRNA expression with time after partial hepatectomy. *$P = 0{\cdot}001$ *versus* before PH. **d** Relative IFN-γ mRNA expression in liver in wild-type (BALB/c) *versus* NKT KO mice before and after PH. *$P = 0{\cdot}037$ *versus* BALB/c mice before PH; †$P = 0{\cdot}044$ *versus* BALB/c 3 h after PH. **e** Effect of treatment with anti-IFN-γ Ab on adhesion scores. *$P = 0{\cdot}020$ *versus* control Ab. **f** Comparison of adhesion score in wild-type (BALB/c) and IFN-γ KO mice. *$P = 0{\cdot}002$ *versus* BALB/c. Values are mean(s.d.) and Student's *t* test was used for all statistical analysis ($n = 5$ per group in all experiments)

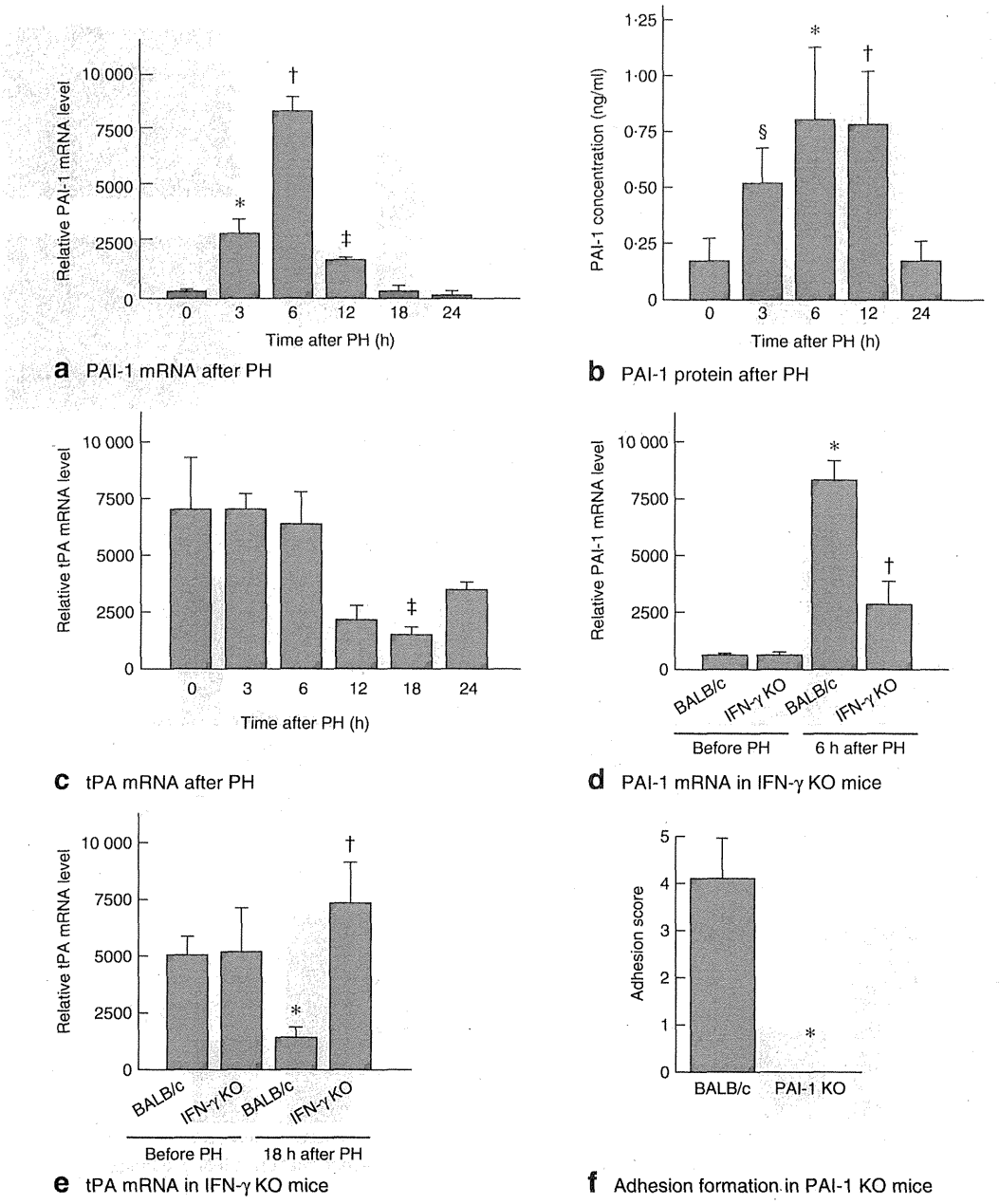

Fig. 3 Role of plasminogen activator inhibitor (PAI) 1, regulated by interferon (IFN) γ, in adhesion formation after partial hepatectomy (PH). **a–c** At the indicated times after PH in BALB/c mice, relative **a** PAI-1 and **c** tissue plasminogen activator (tPA) mRNA expression in the remnant liver were measured by real-time polymerase chain reaction, and **b** plasma levels of the active form of PAI-1 protein were measured by enzyme-linked immunosorbent assay. *$P < 0{\cdot}010$, †$P < 0{\cdot}005$, ‡$P < 0{\cdot}050$ and §$P < 0{\cdot}001$ *versus* before PH. **d** Relative PAI-1 mRNA levels in liver of IFN-γ knockout (KO) and wild-type (BALB/c) mice before and after PH. *$P = 0{\cdot}006$ *versus* BALB/c mice before PH, †$P = 0{\cdot}044$ *versus* BALB/c mice 6 h after PH. **e** Relative tPA mRNA levels in liver of IFN-γ KO and wild-type (BALB/c) mice before and after PH. *$P = 0{\cdot}007$ *versus* BALB/c mice before PH; †$P = 0{\cdot}008$ *versus* BALB/c mice 18 h after PH. **f** Adhesion formation in PAI-1 KO mice compared with wild-type (BALB/c) mice 7 days after PH. *$P = 0{\cdot}002$ *versus* BALB/c mice. Values are mean(s.d.) and Student's *t* test was used for all statistical analysis ($n = 5$ per group in all experiments)

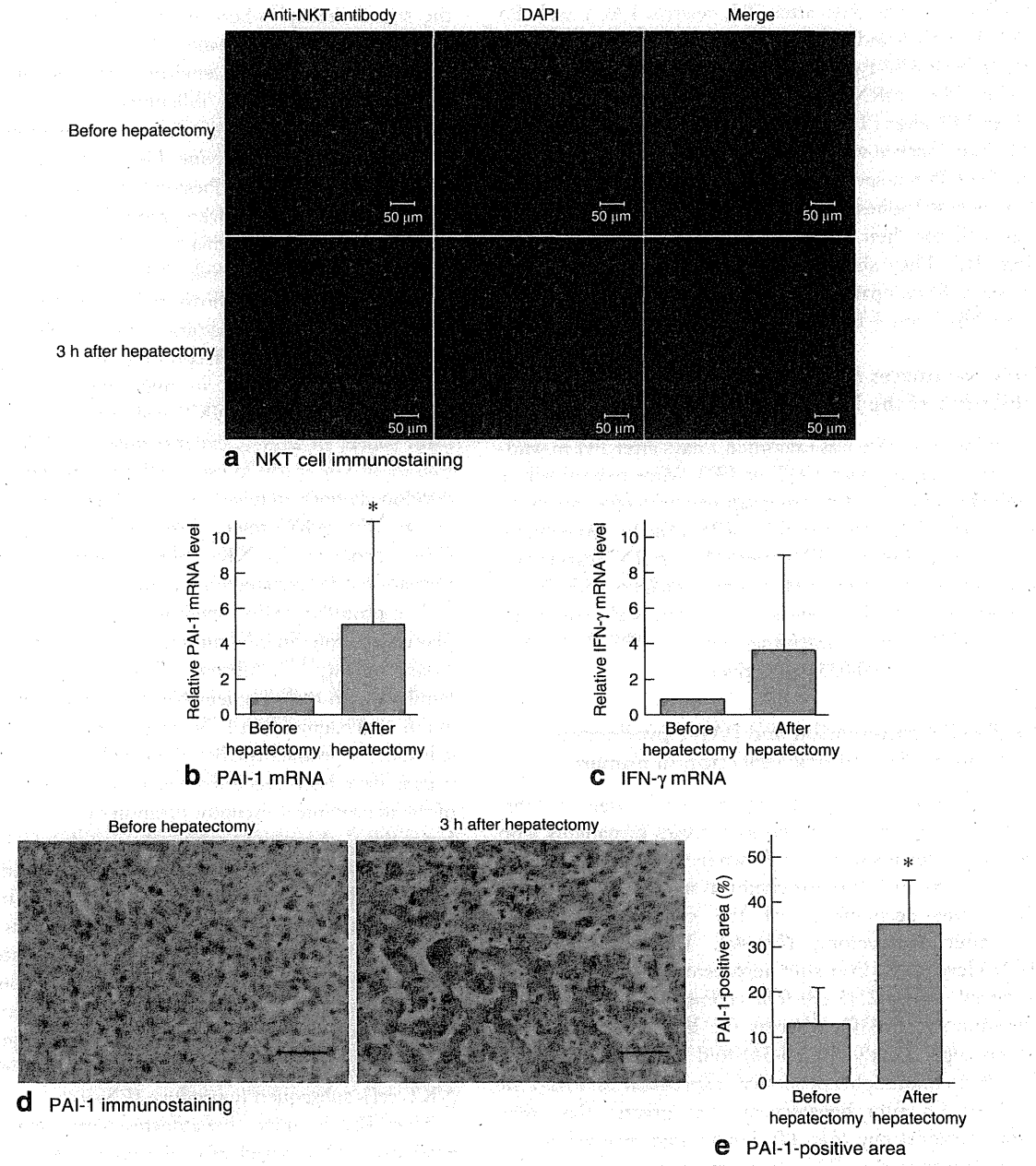

Fig. 4 Natural killer T (NKT) cell accumulation and plasminogen activator inhibitor (PAI) 1 production in liver after hepatectomy in humans. **a** Immunohistochemical staining with anti-NKT (NKT cells, green, left), 4,6-diamidine-2-phenylindole dihydrochloride (DAPI) (blue, middle) and merged images (right) of human liver samples before operation (upper row) and 3 h after the beginning of hepatectomy (lower row). **b**,**c** Relative mRNA levels of **b** PAI-1 and **c** interferon (IFN) γ in the liver before and after hepatectomy ($n = 11$). *$P = 0{\cdot}030$ *versus* before hepatectomy. **d** PAI-1 immunostaining in human liver samples taken before and 3 h after hepatectomy (scale bar 50 μm). **e** Quantification of representative PAI-1 immunostained area in any five high-power fields. *$P < 0{\cdot}001$ *versus* before hepatectomy. Values are mean(s.d.) and Student's *t* test was used for all statistical analysis

To examine the relationship between IFN-γ and PAI-1 production in the liver after PH, relative PAI-1 and tPA mRNA levels 6 and 18 h respectively after PH were examined in both wild-type and IFN-γ KO mice (*Fig. 3d,e*). The level of PAI-1 mRNA in IFN-γ KO mice was significantly reduced 6 h after PH, and that of tPA mRNA was increased at 18 h, compared with levels in wild-type mice ($P = 0{\cdot}044$ and $P = 0{\cdot}008$ respectively). To determine whether PAI-1 also mediated adhesion in this model, PAI-1 KO mice were evaluated for their capacity to develop adhesions 7 days after PH. They showed significantly reduced adhesions (all score 0) compared with the wild-type mice (adhesion score 0(0) *versus* 4·1(0·8); $P = 0{\cdot}002$) (*Fig. 3f*).

HGF attenuates adhesion formation through inhibition of the IFN-γ–PAI-1 pathway

The adhesion score was examined 7 days after PH in wild-type mice treated with HGF or PBS. Mice treated with a single injection of HGF had a significantly lower adhesion score than those treated with PBS (*Fig. S3*, supporting information). Relative IFN-γ and PAI-1 mRNA expression was significantly decreased in mice injected with HGF, whereas tPA mRNA levels were increased, compared with levels in control mice that received PBS ($P < 0{\cdot}001$, $P = 0{\cdot}002$ and $P = 0{\cdot}035$ respectively).

NKT cell accumulation and PAI-1 production in the liver after hepatic resection in humans

Liver specimens from 11 patients were used for this study. Clinicopathological characteristics of patients who underwent hepatectomy are shown in *Table S1* (supporting information). Immunohistochemical staining revealed that NKT cells accumulated at the cut surface of the liver after hepatectomy (*Fig. 4a*). The relative PAI-1 mRNA level in the liver after hepatectomy was significantly increased by 5·25(5·18)-fold compared with before operation ($P = 0{\cdot}030$), whereas the level of IFN-γ rose, but not significantly (3·35(5·34)-fold increase; $P = 0{\cdot}327$) (*Fig. 4b,c*). Immunohistochemical expression of PAI-1 in the liver 3 h after hepatectomy was greater than that before hepatectomy (*Fig. 4d*). Under high magnification, it was apparent that PAI-1 was expressed principally by hepatocytes. The imageJ analysis showed a significant increase in the PAI-1-positive area of the liver after hepatectomy compared with before operation (34·8(9·6) *versus* 13·7(8·1) per cent; $P < 0{\cdot}001$) (*Fig. 4e*).

Discussion

Several factors, including damage to the mesothelial layer caused by surgical injury and infection in the abdominal cavity, induce the accumulation of fibrin at the site of injury[12]. Subsequently, various inflammatory cells including macrophages, Th1 cells and NKT cells modify the pathological environment, and fibrous tissue is synthesized following inflammation[6,7]. Many factors, including cytokines, chemokines, coagulation, and the fibrinolytic system involving PAI-1 and tPA or neuropeptides, play a role in adhesion formation[13,14].

Th1 $CD4^+$ T cells were reported to be crucial for abdominal adhesion formation after surgery in a mouse model[6]. In the present study, NKT cells, a subpopulation of $CD4^+$ T cells, were shown to be essential for adhesion formation after hepatectomy. NKT cells are highly enriched in the liver, accounting for 20–40 per cent of hepatic lymphocytes in mice and 10–20 per cent in humans[15]. Because NKT cells are known to be the main source of IFN-γ, experiments were focused on the role of IFN-γ in the present adhesion model. Adhesions developed poorly in mice treated with anti-IFN-γ antibody and in IFN-γ KO mice. Therefore, it is suggested that IFN-γ produced by NKT cells is essential for adhesion formation after hepatectomy in mice.

The proinflammatory peptide substance P is known to play crucial roles in inflammation, cytokine production and wound healing[13,14]. Substance P belongs to the tachykinin family, which includes neurokinins A and B, endokinins A and B, and haemokinin 1. Neurones are the main source of substance P production, but blood cells, skin, gut and other organs have been recognized as other sources. Activation of the neurokinin 1 receptor promotes peritoneal adhesion formation[14]. A previous study[7] showed that $CD4^+$ T cells from wild-type BALB/c mice produced significantly higher levels of IFN-γ than those from NKT KO mice upon stimulation by tachykinins[7]. Moreover, it was reported that NKT cells increased in the liver after hepatectomy[16], and that another factor, the autonomic nervous system, could increase the number of NKT cells in the liver after hepatectomy[17]. Accordingly, it was suggested that tachykinins are produced by hepatectomy, and stimulated NKT cells subsequently produce IFN-γ.

After PH in mice, hepatocytes were stimulated and produced PAI-1, which played a pivotal role in adhesion formation. In specimens obtained from human patients, the number of NKT cells in the resected liver was increased 3 h after hepatectomy. The level of IFN-γ mRNA was moderately (but not significantly) increased, and that of PAI-1 was significantly raised in the resected liver. Immunostaining revealed markedly increased expression of PAI-1 in hepatocytes.

HGF, originally identified and cloned as a potent mitogen for hepatocytes, has roles in anti-inflammation,

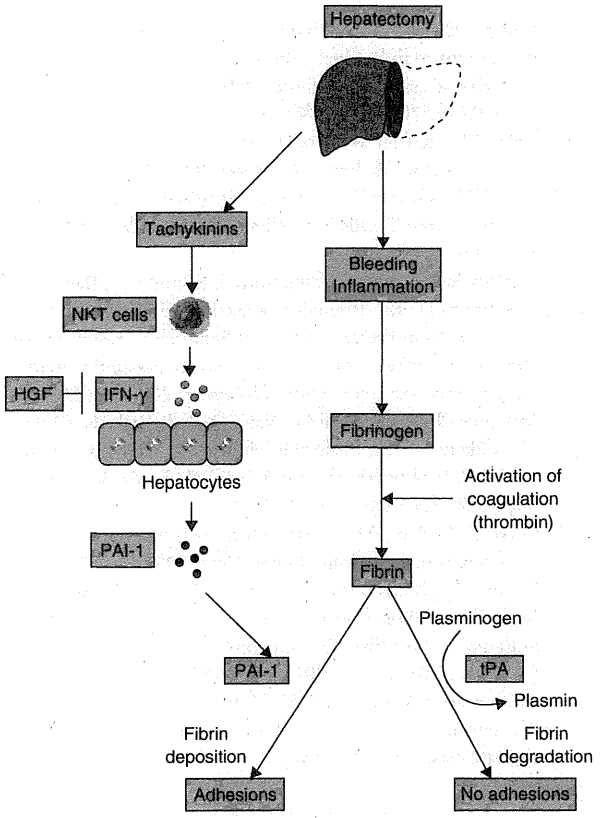

Fig. 5 Proposed role of natural killer T (NKT) cells, interferon (IFN) γ and plasminogen activator inhibitor (PAI) 1 in the induction of adhesion formation after hepatectomy. Bleeding and inflammation are caused by hepatectomy, and then fibrin is formed. Degradation of fibrin depends on the balance between tissue plasminogen activator (tPA) and its inhibitor, PAI-1. On the other hand, after hepatectomy, NKT cell-derived IFN-γ increases the ratio of PAI-1 to tPA leading to fibrin deposition. Hepatocyte growth factor (HGF) protein inhibits adhesion by downregulation of IFN-γ-dependent PAI-1 induction

growth, angiogenesis and antifibrosis[18,19]. It has been reported to suppress IFN-γ expression in an acute graft-*versus*-host disease mouse model[20]. Consistent with previous findings[7], and in the present study, HGF strongly suppressed adhesion formation after hepatectomy by diminishing IFN-γ and PAI-1 production, and increasing tPA production.

The proposed mechanism of adhesion formation after hepatectomy is shown in *Fig. 5*. Although molecular mechanisms underlying adhesion formation after hepatectomy have been suggested, several issues remain. Mechanisms by which IFN-γ influences the PAI-1–tPA balance are unknown. It is also unclear whether or not NKT cells express c-Met, the HGF receptor, and therefore how HGF suppresses IFN-γ production. Recently, Chaturvedi and colleagues[21] reported that a newly developed ultrapure alginate gel decreased the incidence of postoperative adhesion formation in a rat model. It was suggested that this gel can form a fine barrier over injured tissue. Fibrin formation occurred on the injured caecum or peritoneum in that animal model, but fibrin band formation between an injured organ and another organ might also be inhibited by this fine gel. Although generalized cytokine activation seemed to play a pivotal role in abdominal adhesion formation in the present study, Chaturvedi and co-workers' findings suggested that localized covering of injured tissue was effective in inhibiting adhesion formation. Human liver samples retrieved during hepatectomy were analysed here, but it is unclear whether abdominal adhesions developed in these patients. This issue warrants further investigation in clinical studies.

Acknowledgements

The authors thank H. Tsubouchi, Kagoshima University Graduate School of Medical and Dental Sciences, for providing the recombinant HGF protein. This study was supported by JSPS KAKENHI (grant number 22390250). *Disclosure:* The authors declare no conflict of interest.

References

1 Olthof KM, Abecassis MM, Emond JC, Kam I, Merion RM, Gillespie BW *et al.*; Adult-to-Adult Living Donor Liver Transplantation Cohort Study Group. Outcome of adult living donor liver transplantation: comparison of the adult–adult living donor living transplantation cohort study and the national experience. *Liver Transpl* 2011; **17**: 789–797.
2 Ellis H, Moran BJ, Thompson JN, Parker MC, Wilson MS, Menzies D *et al.* Adhesion-related hospital readmissions after abdominal and pelvic surgery: a retrospective cohort study. *Lancet* 1999; **353**: 1476–1480.
3 Ray NF, Denton WG, Thamer M, Henderson SC, Perry S. Abdominal adhesiolysis: inpatient care and expenditure in the United States in 1994. *J Am Coll Surg* 1998; **186**: 1–9.
4 Antoniou A, Lovegrove RE, Tilney HS, Heriot AG, John TG, Rees M *et al.* Meta-analysis of clinical outcome after first and second liver resection for colorectal metastases. *Surgery* 2007; **141**: 9–18.
5 Ghobrial RM, Freise CE, Trotter JF, Tong L, Ojo AO, Fair JH *et al.*; A2ALL Study Group. Donor morbidity after living donation for liver transplantation. *Gastroenterology* 2008; **135**: 468–476.
6 Chung DR, Chitnis T, Panzo RJ, Kasper DL, Sayegh MH, Tzianabos AO. $CD4^+$ T cells regulate surgical and

postinfectious adhesion formation. *J Exp Med* 2002; **195**: 1471–1478.
7 Kosaka H, Yoshimoto T, Yoshimoto T, Fujimoto J, Nakanishi K. Interferon-gamma is a therapeutic target molecule for prevention of postoperative adhesion formation. *Nat Med* 2008; **14**: 437–441.
8 Kilkenny C, Browne WJ, Cuthill IC, Emerson M, Altman DG. Improving bioscience research reporting: the ARRIVE guidelines for reporting animal research. *PLoS Biol* 2010; **8**: e1000412.
9 Yoshimoto T, Paul WE. $CD4^{pos}$, $NK1.1^{pos}$ T cells promptly produce interleukin 4 in response to *in vivo* challenge with anti-CD3. *J Exp Med* 1994; **179**: 1285–1295.
10 Kato J, Okamoto T, Motoyama H, Uchiyama R, Kirchhofer D, Van Rooijen N *et al.* Interferon-gamma-mediated tissue factor expression contributes to T-cell-mediated hepatitis through induction of hypercoagulation in mice. *Hepatology* 2013; **57**: 362–372.
11 Holmdahi L. The role of fibrinolysis in adhesion formation. *Eur J Surg Suppl* 1997; **163**: 24–31.
12 diZerega G, Campeau JD. Peritoneal repair and post-surgical adhesion formation. *Hum Reprod Update* 2001; **7**: 547–555.
13 Schäffer M, Beiter T, Becker HD, Hunt TK. Neuropeptides: mediators of inflammation and tissue repair? *Arch Surg* 1998; **133**: 1107–1116.
14 Reed KL, Heydrick SJ, Aarons CB, Prushik S, Gower AC, Stucchi AF *et al.* A neurokinin-1 receptor antagonist that reduces intra-abdominal adhesion formation decreases oxidative stress in the abdomen. *Am J Physiol Gastrointest Liver Physiol* 2007; **293**: 544–551.
15 Exley MA, Koziel MJ. To be or not to be NKT: natural killer T cells in the liver. *Hepatology* 2004; **40**: 1033–1040.
16 Abo T, Kawamura T, Watanabe H. Physiological responses of extrathymic T cells in the liver. *Immunol Rev* 2000; **174**: 135–149.
17 Minagawa M, Oya H, Yamamoto S, Shimizu T, Bannai M, Kawamura H *et al.* Intensive expansion of natural killer T cells in the early phase of hepatocyte regeneration after partial hepatectomy in mice and its association with sympathetic nerve activation. *Hepatology* 2000; **31**: 907–915.
18 Miyazawa K, Tsubouchi H, Naka D, Takahashi K, Okigaki M, Arakaki N *et al.* Molecular cloning and sequence analysis of cDNA for human hepatocyte growth factor. *Biochem Biophys Res Commun* 1989; **163**: 967–973.
19 Boros P, Miller CM. Hepatocyte growth factor: a multifunctional cytokine. *Lancet* 1995; **345**: 293–295.
20 Kuroiwa T, Kakishita E, Hamano T, Kataoka Y, Seto Y, Iwata N *et al.* Hepatocyte growth factor ameliorates acute graft-*versus*-host disease and promotes hematopoietic function. *J Clin Invest* 2001; **107**: 1365–1373.
21 Chaturvedi AA, Lomme RM, Hendriks T, van Goor H. Prevention of postsurgical adhesions using an ultrapure alginate-based gel. *Br J Surg* 2013; **100**: 904–910.

Supporting information

Additional supporting information may be found in the online version of this article:

Fig. S1 Liver sections from wild-type mice 1, 3, 5 and 7 days after hepatic resection, stained with haematoxylin and eosin and Sirius red (Word document)

Fig. S2 Fibrin deposition 3 h and 1 day after partial hepatectomy in mice (Word document)

Fig. S3 Effect of hepatocyte growth factor on development of adhesions and the interferon γ–plasminogen activator inhibitor 1 pathway (Word document)

Table S1 Clinicopathological data for the 11 patients included in this study (Word document)

Immunobiology 220 (2015) 74–82

Contents lists available at ScienceDirect

Immunobiology

journal homepage: www.elsevier.com/locate/imbio

PolyI:C and mouse survivin artificially embedding human 2B peptide induce a CD4+ T cell response to autologous survivin in HLA-A*2402 transgenic mice

Jun Kasamatsu[a,1], Shojiro Takahashi[a,b,1], Masahiro Azuma[a,1,2], Misako Matsumoto[a], Akiko Morii-Sakai[a], Masahiro Imamura[b], Takanori Teshima[b], Akari Takahashi[c], Yoshihiko Hirohashi[c], Toshihiko Torigoe[c], Noriyuki Sato[c], Tsukasa Seya[a,*]

[a] Department of Microbiology and Immunology, Hokkaido University Graduate School of Medicine, Kita-ku, Sapporo, Japan
[b] Department of Hematology, Hokkaido University Graduate School of Medicine, Kita-ku, Sapporo, Japan
[c] Department of Pathology, Sapporo Medical University School of Medicine, Chuoh-ku, Sapporo, Japan

ARTICLE INFO

Article history:
Received 28 March 2014
Received in revised form 4 August 2014
Accepted 6 August 2014
Available online 23 August 2014

Keywords:
Survivin
PolyI:C
CD4 epitope
Peptide vaccine
Th1 response
Interferon-γ
Tumor immunity

ABSTRACT

$CD4^+$ T cell effectors are crucial for establishing antitumor immunity. Dendritic cell maturation by immune adjuvants appears to facilitate subset-specific $CD4^+$ T cell proliferation, but the adjuvant effect for CD4 T on induction of cytotoxic T lymphocytes (CTLs) is largely unknown. Self-antigenic determinants with low avidity are usually CD4 epitopes in mutated proteins with tumor-associated class I-antigens (TAAs). In this study, we made a chimeric version of survivin, a target of human CTLs. The chimeric survivin, where human survivin-2B containing a TAA was embedded in the mouse survivin frame (MmSVN2B), was used to immunize HLA-A-2402/K^b-transgenic (HLA24^b-Tg) mice. Subcutaneous administration of MmSVN2B or xenogeneic human survivin (control HsSNV2B) to HLA24^b-Tg mice failed to induce an immune response without co-administration of an RNA adjuvant polyI:C, which was required for effector induction *in vivo*. Although HLA-A-2402/K^b presented the survivin-2B peptide in C57BL/6 mice, 2B-specific tetramer assays showed that no $CD8^+$ T CTLs specific to survivin-2B proliferated above the detection limit in immunized mice, even with polyI:C treatment. However, the $CD4^+$ T cell response, as monitored by IFN-γ, was significantly increased in mice given polyI:C + MmSVN2B. The Th1 response and antibody production were enhanced in the mice with polyI:C. The CD4 epitope responsible for effector function was not $Hs/MmSNV_{13\text{-}27}$, a nonconserved region between human and mouse survivin, but region 53-67, which was identical between human and mouse survivin. These results suggest that activated, self-reactive $CD4^+$ helper T cells proliferate in MmSVN2B + polyI:C immunization and contribute to Th1 polarization followed by antibody production, but hardly participate in CTL induction.

Introduction

Dendritic cells (DCs) present exogenous antigens (Ags) to cells in the major histocompatibility complex (MHC) class I-restricted Ag-presentation pathway and cause the proliferation of $CD8^+$ T cells specific to the extrinsic Ag. When tumor cells have soluble and insoluble exogenous Ags, MHC class I Ag presentation is mainly transporter associated with antigen processing (TAP)- and proteasome-dependent, suggesting the pathway is partly shared with the pathway for endogenous Ag presentation. The delivery of exogenous Ag by DCs to the pathway for MHC class I-restricted Ag presentation is called cross-presentation (Bevan 1976).

PolyI:C is a double-stranded RNA analog that activates RNA-sensing pattern-recognition receptor pathways (Matsumoto and Seya 2008; Seya and Matsumoto 2009). PolyI:C is an efficient trigger of cross-presentation, and facilitates cross-priming of $CD8^+$ T cells in the presence of Ag. Tumor-associated antigens (TAAs) usually expressed in low levels are thought to need support from pattern-recognition receptor activation to induce TAA-specific cytotoxic T lymphocytes (CTLs) (Seya et al. 2013).

* Corresponding author at: Department of Microbiology and Immunology, Hokkaido University Graduate School of Medicine, Kita 15, Nishi 7, Kita-ku, Sapporo 060-8638, Japan. Tel.: +81 11 706 7866; fax: +81 11 706 7866.
E-mail address: seya-tu@pop.med.hokudai.ac.jp (T. Seya).
[1] These authors equally contributed.
[2] Present address: University of Montreal, 2900 Edouard-Montpetit, Faculty of Medicine/Pavilion Roger Gaudry, Department of Pathology and Cellular Biology, Montreal, QC, H3T 1J4, Canada.

http://dx.doi.org/10.1016/j.imbio.2014.08.017
0171-2985/

Many TAAs have been identified and tested for tolerability to patients and for ability to suppress tumor progression. Peptide vaccine immunotherapy against cancer has been studied clinically (Rosenberg et al. 2004). Survivin (SVN) is a TAA that generates CTLs in cancer patients (Schmitz et al. 2000; Andersen et al. 2001). Human survivin (HsSVN) is a 16.5 kDa cytoplasmic protein that inhibits caspase 3 and 7 in cells stimulated to undergo apoptosis (Altieri 2001). SVN is a member of the inhibitor of apoptosis protein family associated with fetal development. Therefore, except for testis, thymus and placenta, normal tissues express little SVN (Ambrosini et al. 1997; Altieri 2001). SVN is required in early thymocyte development from CD4/CD8-double-negative cells to CD4/CD8-double-positive lymphocytes (Okada et al. 2004). SVN is expressed in a wide variety of malignant cells (Altieri 2001; Fukuda and Pelus 2006). There are several splicing variants including a variant HsSVN2B with a cryptic epitope for MHC class I in humans. An HsSVN2B peptide (AYACNTSTL: 80–88) is an HLA-A*2402-restricted peptide recognized by CD8+ CTLs (Hirohashi et al. 2002). Some cancer cells have higher mRNA levels of the HsSVN splice variant 2B, but whether this splice variant functions in tumorigenesis is unknown (Li 2005).

Several trials have studied the SVN2B peptide in cancer patients (Tsuruma et al. 2008; Honma et al. 2009; Kameshima et al. 2013). Although CTLs specific for SVN were detected in peripheral blood mononuclear cells of most cancer patients, as determined by HLA-A*2402/SVN2B tetramer assays, no substantial therapeutic effect on cancer is seen in most clinical studies. A phase I clinical study found that vaccination with SVN2B peptide combined with IFN-α had significant therapeutic benefits in advanced pancreatic cancer patients, in spite of IFN-mediated side effects. Thus, an IFN-inducing adjuvant, that simultaneously up-regulates Ag-presentation and IFN-inducible genes, might more efficiently contribute to the clinical benefits of SVN for cancer patients.

PolyI:C is an analog of virus double-stranded RNA with IFN-inducing adjuvant properties. To test the effect of polyI:C on survivin-derived CTLs, we used a mouse model expressing human HLA-A24 that presents the SVN2B peptide (Gotoh et al. 2002). Mice have no splice counterpart for HsSVN2B and therefore mouse survivin (MmSVN) lacks the 2B portion of HsSVN, although the mouse ortholog is 84% homologous to HsSVN (Kobayashi et al. 1999). When BALB/c mice are injected intraperitoneally with HsSVN2B + RNA adjuvant, high levels of $CD4^+$ T cells are induced in splenic T cells, as determined by IFN-γ, TNF-α, and IL-2 production, as well as development of lytic MHC class II-restricted T cells and memory (Charalambous et al. 2006).

The N-terminal sequence of HsSVN, which includes amino acids 13–27 (FLKDHRISTFKNWPF), differs from that of MmSVN (YLKNYRIATFKNWPF) (Charalambous et al. 2006). Therefore, high frequencies of self-reactive $CD4^+$ T cells specific for a tumorigenic protein might be elicited in mice with xenogeneic HsSVN. However, self-reactive $CD4^+$ T cells can be induced toward syngeneic or nonmutated CD4 epitopes in cancer patients (Topalian et al. 1996; Osen et al. 2010). To test the possibility that sub-derived self-CD4 epitopes participate in $CD8^+$ CTL proliferation, we made a chimeric survivin protein (MmSVN2B), where the human 2B exon sequence was embedded into MmSVN. We immunized HLA-A-2402/K^b-transgenic (HLA24^b-Tg) B6 mice with MmSVN2B. The results indicated that the $CD8^+$ CTL response to a self-tumor Ag (2B peptide) was barely enhanced by treatment of HLA24^b-Tg mice with MmSVN2B in the presence of polyI:C. However, $CD4^+$ T cell immune responses to the CD4 epitope of MmSVN2B and HsSVN2B were significantly enhanced in HLA24^b-Tg mice with SVN2B proteins + polyI:C. The CD4 epitopes were not the N-terminal $HsSVN_{13-27}$ and $MmSVN_{13-27}$ sequences, but the $Hs/MmSVN_{53-67}$ (DLAQCFFCFKELEGW) sequence, which is identical in HsSVN2B and MmSVN2B and thus a nonmutated CD4 epitope. PolyI:C was required for proliferation of self-reactive $CD4^+$ Th1 cells that recognized the syngeneic epitope. We discuss how RNA adjuvant might induce $CD4^+$ Th1 cells and act in the antitumor immune response.

Materials and methods

Bioinformatics analysis

Ensembl databases (http://asia.ensembl.org/index.html) were used to investigate human and mouse SVN genomic structure. Primate and rodent short interspersed nuclear elements (SINEs) were predicted using the Repeat Masker program (http://www.repeatmasker.org/). Results from databases were confirmed by comparison to previous reports (Mahotka et al. 1999).

Expression analysis

Total RNA was extracted from tissues from C57BL/6 mice and murine cell lines using RNeasy Mini Kits (Qiagen) following the manufacturer's instructions. RT-PCR used High Capacity cDNA Reverse Transcription Kits (Applied Biosystems) according to the manufacturer's instructions. Primer pairs were designed to span separate exons to avoid amplifying other genomic DNA. Primers were 5′-ACTACCGCATCGCCACCT-3′ (forward) and 5′-GCTTGTTGTTGGTCTCCTTTG-3′ (reverse) for detection of the murine SVN gene (MmSVN) and 5′-TGTAACCAACTGGGACGATAT-3′ (forward) and 5′-CTTTTCACGGTTGGCCTTAG-3′ (reverse) for murine *Gapdh*. PCR conditions for mSVN were 94 °C 3 min; 35 cycles of 94 °C 30 s, 65 °C 30 s, 72 °C for 30 s; and 7 min 72 °C. *Gapdh* PCR conditions were 94 °C 3 min; 30 cycles of 94 °C 30 s, 65 °C 30 s, and 72 °C 30 s; and 7 min at 72 °C.

Antigens

The HsSVN2B-coding sequence was amplified using primers 5′-CGGGATCCATGGGTGCCCCGACG-3′ (underline: *Bam*HI site) and 5′-GGAATTCTCAATCCATGGCAGC-3′(underline: *Eco*RI site). To construct the mSVN 2B gene (MmSVN2B), we used two-step PCR to make a chimeric gene of the mSVN gene and the human 2B exon (Fig. 2). In the first PCR, two fragments containing exon 1–2 and exon 3–4 were amplified using primers 5′-CCGCTCGAGATGGGAGCTCCGGCGCT-3′ (underline: *Xho*I site) and 5′-*ACCGTGCCCGGCCCA*ATCGGGTTGTCA-3′ (italics: 5′-end of exon 2B of the HsSVN2B gene) for exon 1 and exon 2 and 5′-*GGGCGGATCACGAG*AGAGGAGCATAGAAAGCA-3′ (italics: 3′-end of exon 2B) and 5′-CGGGATCCTTAGGCAGCCAGCTGCTCAAT-3′ (underline: *Bam*HI site) for exon 3 and exon 4. The exon 2B fragment was amplified using primers 5′-*CGATGACAACCCGATT*GGGCCGGGCACGG-3′ (italics: 3′-end of exon 1 and exon 2 of MmSVN) and 5′-*TTTCTATGCTCCTCT*CTCGTGATCCGCCC-3′ (italics: 5′-end of exon 3 and exon 4 of MmSVN). In the second PCR, the three templates from the first PCR were mixed in equal amounts and amplified using primers 5′-CCGCTCGAGATGGGAGCTCCGGCGCT-3′ (underline: *Xho*I site) and 5′-CGGGATCCTTAGGCAGCCAGCTGCTCAAT-3′ (underline: *Bam*HI site). The pCold vector II (TaKaRa) and SVN fragments were restriction digested and ligated overnight with T4 ligase (Promega) at 4 °C. Ligation mixtures were transformed into competent *Escherichia coli* strain BL21 (DE3) cells. After preculturing for 2 h at 37 °C, cells were cooled on ice. Recombinant protein expression was induced with isopropyl-1-thio-β-D-galactopyranoside at a final concentration of 1 mM and cultured for 24 h at 16 °C. N-His-tagged survivin proteins were purified using a Profinia protein purification system (Biorad). Buffer of

purified SVN proteins was sequentially exchanged with PBS containing 2 M urea. To rule out lipopolysaccharide contamination, we treated survivin proteins with 200 μg/ml of polymixin B (Sigma) for 30 min at 37 °C before use. OVA (ovalbumin) (Sigma) was similarly treated with polymixin B as an Ag.

Mice

C57BL/6 (H-2b) mice were from Clea Japan (Tokyo). HLA24^b-Tg was from SLC Japan (Gotoh et al. 2002). Mice were maintained in the Hokkaido University Animal Facility (Sapporo, Japan) in specific pathogen-free conditions. All experiments used mice that were 8–12 weeks old at the time of first procedure. All mice were used according to the guidelines of the institutional animal care and use committee of Hokkaido University, which approved this study (ID number: 08-0243, "Analysis of immune modulation by toll-like receptors").

Reagents, antibodies and cells

PolyI:C and $OVA_{323-339}$ peptide (ISQAVHAAHAEINEAGR) were from Sigma. $OVA_{257-264}$ peptide (SIINFEKL: SL8), OVA (H2 K^b-SL8), HLA-A*2402 survivin-2B and HIV tetramer were from MBL. SVN2B peptide (AYACNTSTL) and HLA-A*2402/2B peptide-restricted human T cell clones (Idenoue et al. 2005) were kindly provided by Dr. Noriyuki Sato (Department of Pathology, School of Medicine, Sapporo Medical University). Human and murine-specific helper peptides (Charalambous et al. 2006) $MmSVN_{13-27}$ (YLKNYRIATFKNWPF) and Hs SVN_{13-27} (FLKDHRISTFKNWPF) and the common helper peptide Hs/Mm SVN_{53-67} (DLAQCFFCFKELEGW), were synthesized by Biologica Co. Ltd (Nagoya). Peptide purity was >95%. To eliminate lipopolysaccharide contamination, all peptides were treated with 200 μg/ml polymixin B (Sigma) for 30 min at 37 °C before use (Nishiguchi et al. 2001). Anti-CD3ε (145-2C11), anti-CD8α (53-6.7) and anti-IFNγ (XMG1.2) antibodys (Abs) were from BioLegend. Anti-CD4 Ab (L3T4) was from eBiosciences and ViaProbe was from BD Biosciences. Dendritic cells were prepared from spleens of mice as described previously (Azuma et al., 2012).

Antigen-specific T cell expansion in vivo

HLA24^b Tg mice (Gotoh et al. 2002) were subcutaneously immunized with 100 μg of each antigen and 100 μg poly I:C once a week for 4 weeks. After 7 days from the last immunization, spleens were extracted, homogenized and stained with FITC-CD8α and PE-OVA (Azuma et al. 2012) or PE-SVN2B tetramer for detecting antigen-specific CD8$^+$ T cells (Tsuruma et al. 2008). For intracellular cytokine detection, splenocytes were cultured with 100 nM SL8 or survivin 2B peptide for 6 h with 10 μg/ml brefeldin A (Sigma–Aldrich) added in the last 4 h. For intracellular cytokine detection of antigen-specific CD4$^+$ T cells, splenocytes were cultured with 100 nM $OVA_{323-339}$ peptide or SVN helper peptide for 6 h with 10 μg/ml brefeldin A (Sigma–Aldrich) added in the last 5 h. Cells were stained with PE-anti-CD8α/FITC-anti-CD3ε for CD8$^+$ T cells or PE-anti-CD4/FITC-anti-CD3ε for CD4$^+$ T cells. After cell-surface staining, cells were fixed and permeabilized with Cytofix/Cytoperm (BD Biosciences) according to the manufacturer's instruction. Fixed and permeabilized cells were stained with APC-anti-IFN-γ. Stained cells were analyzed with FACSCalibur (BD Biosciences) and FlowJo software (Tree Star) (Azuma et al. 2012).

ELISA

Sera were collected from immunized mice once a week for 4 weeks and 96-well plates were coated with 10 μg/ml OVA, MmSVN2B and HsSVN2B in ELISA/ELISPOT coating buffer (eBioscience) and incubated overnight at 4 °C. ELISA diluent solution (eBioscience) was used for blocking and antibody dilution. PBS with 0.05% Tween 20 was used for washes. Anti-OVA or anti-SVN in sera was assessed by ELISA using antiserum for IgG2a/b and IgG1 diluted 1000-fold and 10,000-fold and incubated for 2 h at room temperature. After washing, isotype IgGs were detected using goat anti-mouse total IgG, IgG1, or IgG2a conjugated to HRP (Southern Biotechnology Associates). After washing, plates were stained with 1XTMB ELISA substrate solution (eBioscience) and reactions stopped with 2 N H_2SO_4 before measuring absorbance.

Statistical analyses

For comparison of two groups, *P*-values were calculated with a Student's *t*-test. For comparison of multiple groups, P-values were calculated with one-way analysis of variance (ANOVA) with Bonferroni's test. Error bars are SD or SEM between samples.

Results

Origin of human SVN exon 2B

The HsSVN gene has four conserved and two cryptic exons (Mahotka et al. 1999). The authentic HsSVN gene encode 142 amino acids in exons 1–4. On the other hand, the HsSVN2B product is 165 amino acids encoded by exons 1, 2, 2B, 3 and 4. Exon 2B is hidden within intron 2, which is spliced into mature HsSVN2B mRNA in-frame between exons 2 and 3 (Mahotka et al. 1999). Exon 2B is followed by the GT-AG role and expressed in many tumor cells and tumor cell lines, suggesting that splicing predominantly occurs in malignantly transformed cells (Mahotka et al. 2002). According to the Ensembl database, HsSVN intron 2 had two Alu sequences (Fig. 1A), and exon 2B resulted from the second Alu. In contrast, the MmSVN gene had four exons separated by three introns with no Alu sequence in intron 2; instead, MmSVN had several SINE sequences characteristic of rodents in intron 2 (Fig. 1A). Although the exon sequences were conserved in human and mouse SVNs, two intron sequences diverged between human and mouse (Fig. 1A). These results suggested that integration of exon 2B was evolutionarily new and formed after an Alu insertion. Although the SVN gene is conserved in yeast and humans, exon 2B was established after the divergence of human and mouse.

We used RT-PCR to investigate transcripts resulting from splicing other exons around exon 2 into the MmSVN mRNA. Results of mRNAs from mouse organs and cell lines are in Fig. 2B. The results suggested that no alternative exons around exon 2 in the MmSVN gene. We detected a ~200 bp product in most organs and cell lines tested (Fig. 2B), but this was not an MmSVN transcript.

Generation of a mmSVN2B construct

A SVN2B peptide derived from the HsSVN2B gene that contained the exon 2B sequence was recognized by CTLs in cancer patients (Hirohashi et al. 2002; Tsuruma et al. 2008; Honma et al. 2009) and a CTL clone was established from patients (Idenoue et al. 2005). We artificially constructed an MmSVN2B with a xenogeneic human exon 2B inserted into the boundary between exon 2 and 3 of SVN (Fig. 2A and B). Prominent amino acid substitutions between MmSVN2B and HsSVN2B were concentrated in the N-terminal region encoded by exon 1 (Fig. 2B), and a CD4 epitope is in this region (Li 2005; Mahotka et al. 2002). In an earlier paper, this $HsSVN_{13-27}$ region, but not $MmSVN_{13-27}$, was an effective CD4 epitope that promoted $HsSVN_{13-27}$-specific CD4$^+$ T cell proliferation

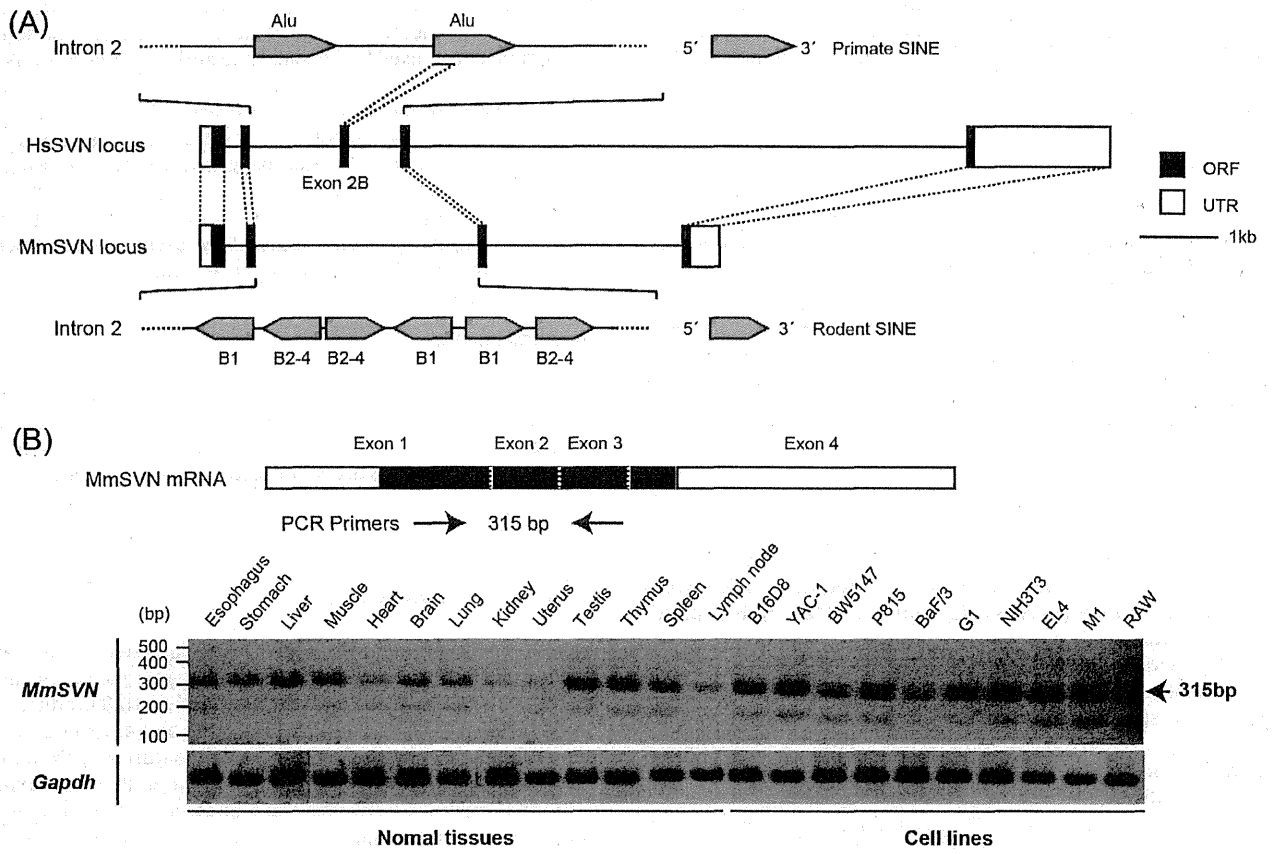

Fig. 1. Genome structure and expression of human and murine SVN gene. (A) Comparison of human and murine survivin gene structure. Survivin gene structures were defined by the Ensembl genome browser. Primate and rodent SINEs were predicted using Repeat Masker program. Filled boxes, coding regions; open boxes, 5′- and 3′-untranslated regions. (B) Structure of murine survivin transcript and RT-PCR analysis of organs and cell lines. Arrows, survivin-detecting PCR primers.

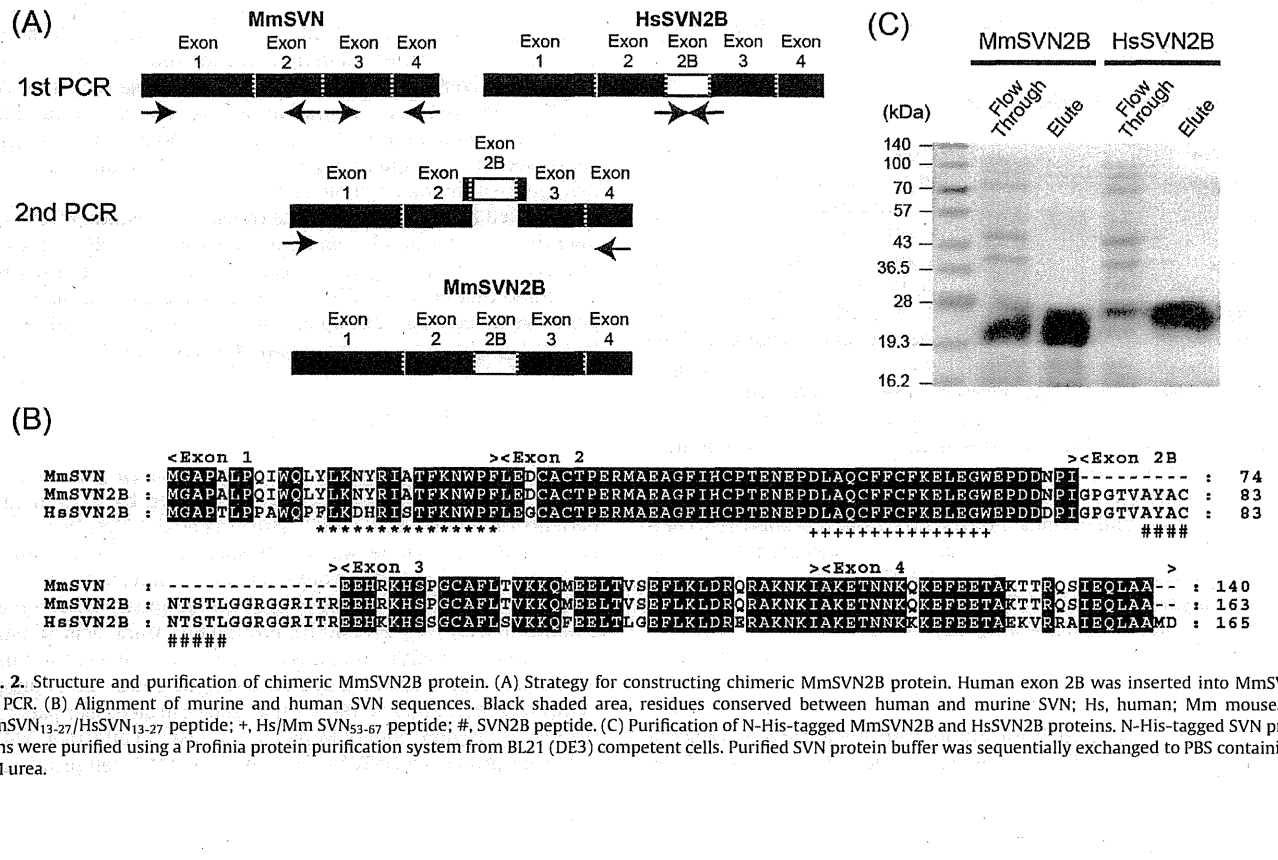

Fig. 2. Structure and purification of chimeric MmSVN2B protein. (A) Strategy for constructing chimeric MmSVN2B protein. Human exon 2B was inserted into MmSVN by PCR. (B) Alignment of murine and human SVN sequences. Black shaded area, residues conserved between human and murine SVN; Hs, human; Mm mouse. *, $MmSVN_{13-27}$/$HsSVN_{13-27}$ peptide; +, Hs/Mm SVN_{53-67} peptide; #, SVN2B peptide. (C) Purification of N-His-tagged MmSVN2B and HsSVN2B proteins. N-His-tagged SVN proteins were purified using a Profinia protein purification system from BL21 (DE3) competent cells. Purified SVN protein buffer was sequentially exchanged to PBS containing 2 M urea.

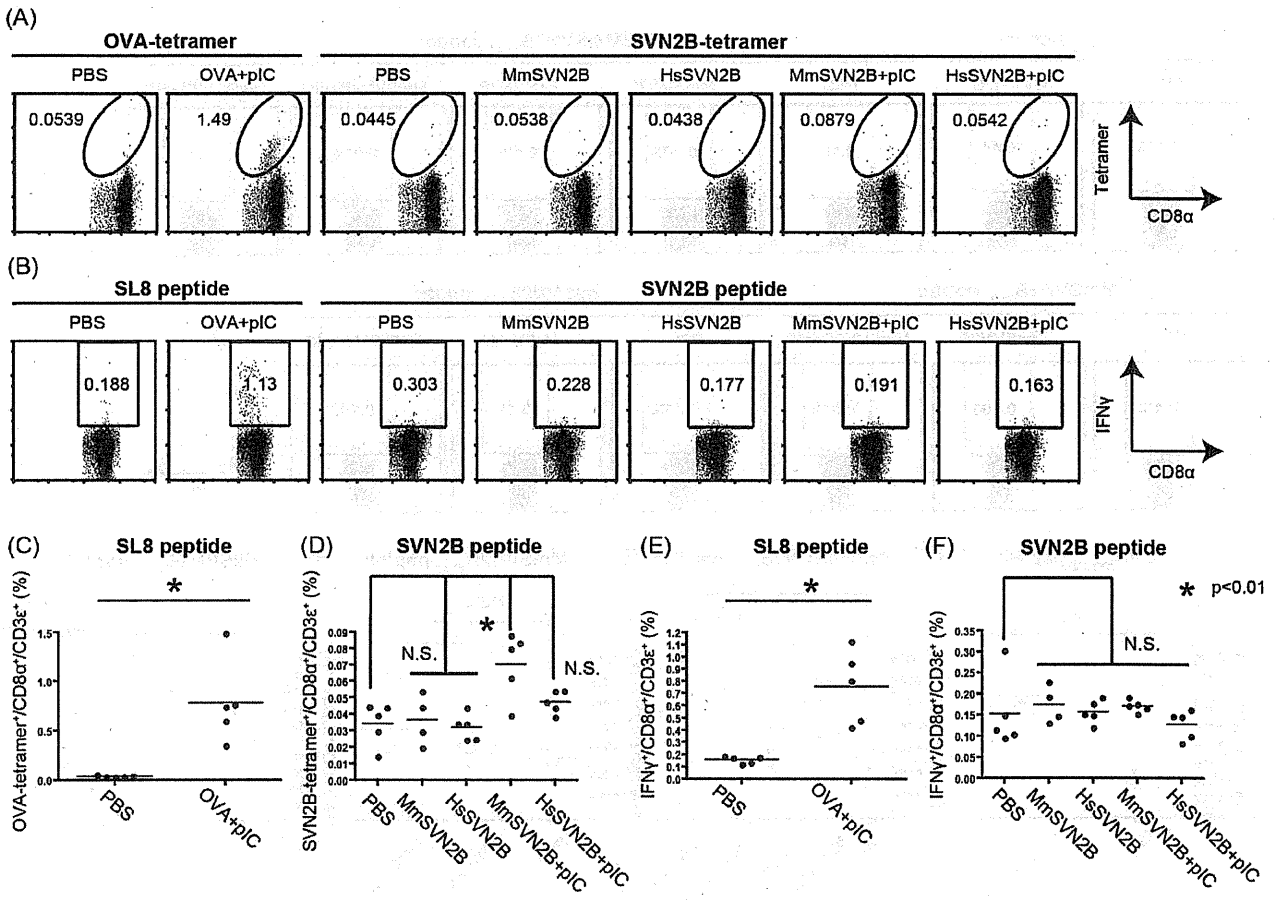

Fig. 3. Expansion of OVA and SVN-specific CD8$^+$ T cells. (A) HLA24^b-Tg mice were immunized with 100 μg antigen and 100 μg poly I:C once a week for 4 weeks. After 7 days from the last immunization, spleens were homogenized and stained with FITC-CD8α and PE-OVA or PE-survivin tetramer to detect antigen-specific CD8$^+$ T cells. (B) Splenocytes were cultured *in vitro* in the presence of SL8 or SVN2B peptides for 6 h and IFN-γ production was measured by FACS. (C, D) Average percentages of OVA-positive and SVN2B-tetramer positive CD8$^+$ T cells shown in (A). (E, F) Average percentages of IFN-γ producing CD8$^+$ T cells specifically in response to SL8 or SVN2B peptide in (B). $^*p < 0.01$.

(Charalambous et al. 2006). His-tagged MmSVN2B and HsSVN2B proteins were purified and used as Ags (Fig. 2C).

CD4$^+$ and CD8$^+$ T cells that react to MmSVN2B plus polyI:C

We examined the ability of MmSVN2B to induce IFN-γ and CD8$^+$ T cell proliferation by immunizing HLA24^b-Tg mice with MmSVN2B or HsSVN2B with or without polyI:C (Fig. 3). SVN2B-specific CTLs were probed by SVN2B-tetramer (Fig. 3A) and IFN-γ staining (Fig. 3B). SVN2B-specific human CD8$^+$ T cells were detected with SVN2B-tetramer (Fig. S1), which enabled us to search for SVN2B-specific CTLs in HLA24^b-Tg mice (Idenoue et al. 2005). Expression of CD40 was up-regulated in CD8α$^+$ conventional DCs to a similar extent with MmSVN2B or HsSVN2B (Fig. S2), consistent with a report on CD40 that promotes cross-priming by Ahonen et al. (J Exp Med, 2004). OVA and polyI:C were used as positive controls (Fig. 3A, B left panels), and SL8 (SIINFEKL)-specific CTLs were monitored with OVA tetramer (Azuma et al. 2012). Both OVA-tetramer-positive and IFN-γ-producing CD8$^+$ T cells were detected in mice immunized with OVA and polyI:C (Fig. 3C, E). Without polyI:C stimulation, only small number of OVA-tetramer-positive cells were upregulated compared to controls (Azuma et al. 2012; Azuma & Seya unpublished data).

When HLA24^b-Tg mice were immunized with MmSVN2B or HsSVN2B without polyI:C, no significant induction of SVN2B-tetramer-positive (Fig. 3D) or IFN-γ-inducing cells was observed (Fig. 3F). When polyI:C was included, only a small increase in SVN2B-tetramer-positive cells was detected in mice given MmSVN + polyI:C with no significant increase in IFN-γ (Fig. 3F). Mice receiving HsSVN + polyI:C (Fig. 3D) or polyI:C alone (not shown) showed no significant increase in SVN2B-specific CD8$^+$ T cells. Consistent with the lack of tetramer-positive CTL induction, MmSVN2B treatment failed to regress MmSVN2B-transfected tumor cells implanted into HLA24^b-Tg mice. In EG7 tumor-bearing mice, administration of polyI:C alone (without Ag) induces tumor-growth retardation due to the contribution of endogenous Ag (Azuma et al. 2012), but in this case with tumor-unloaded mice polyI:C exhibited no tumor-regressing activity (data not shown), possibly due to the lack of Ag.

Next, we determined the amounts of CD4$^+$ T cells that reacted with MmSVN2B. The positive control group received OVA Ag and polyI:C (Fig. 4A, B). The negative control group received PBS without Ag and polyI:C, but basal frequencies of IFN-γ-producing CD4$^+$ T cells were detected in this group even in the absence of polyI:C or Ag (Fig. 4). When MmSVN2B or HsSVN2B only was used to immunize mice, no significant response was seen in CD4$^+$ T cells compared to PBS controls (Fig. 4A, C–E). When polyI:C was included, IFN-γ-producing CD4$^+$ T cells restimulated with Hs/MmSVN$_{53-67}$ peptide increased significantly in mice that received MmSVN and HsSVN (Fig. 4C, D). The sequence of MmSVN$_{53-67}$ was identical to the sequence of HsSVN$_{53-67}$ (Fig. 2B). However, we did not detect a significant increase in IFN-γ-producing CD4$^+$ T cells in mice

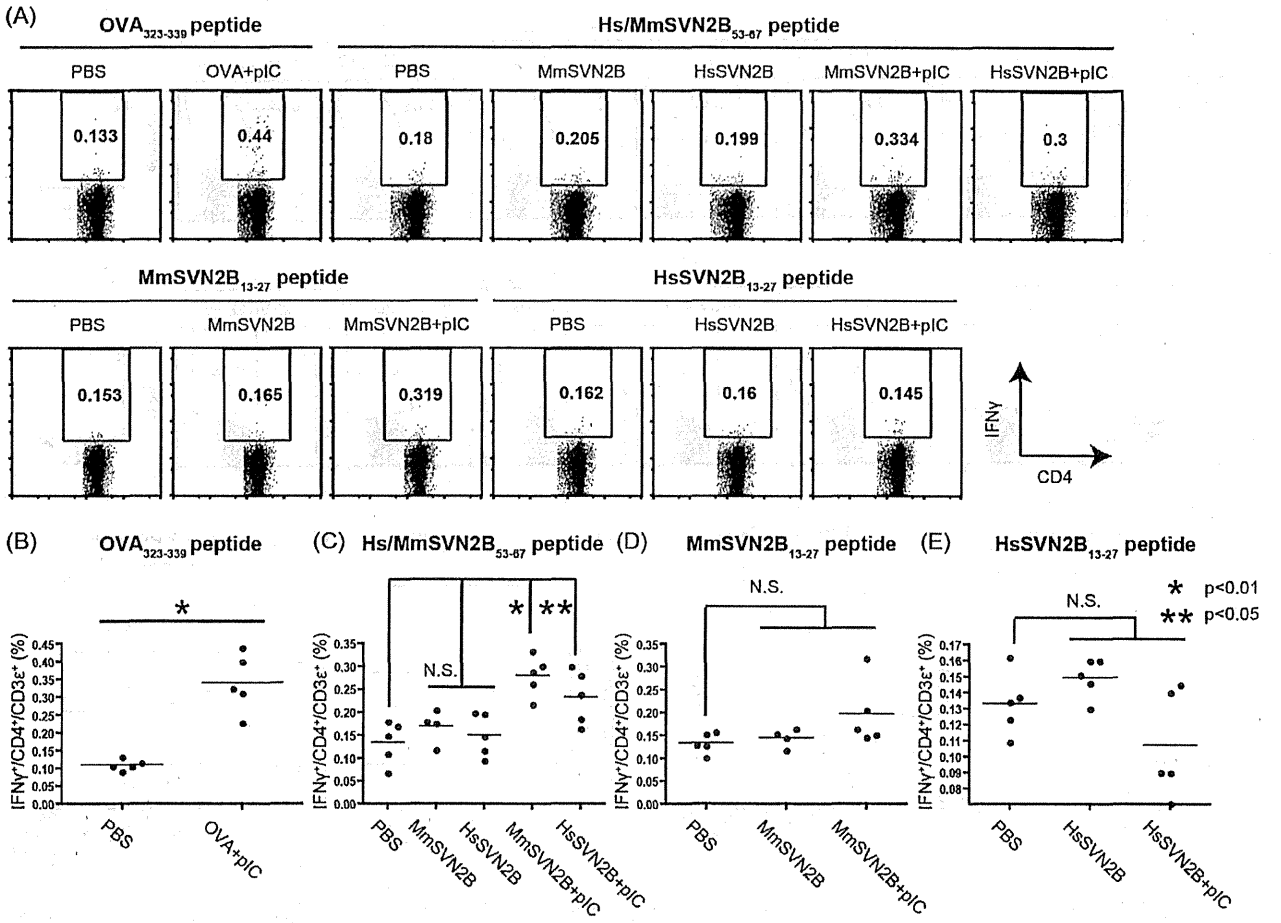

Fig. 4. Expansion of OVA and SVN-specific CD4⁺ T cells. (A) HLA24^b-Tg mice were immunized with 100 μg each antigen and 100 μg poly I:C once a week for 4 weeks. After 7 days from the last immunization, splenocytes were cultured with 100 nM $OVA_{323-339}$ peptide or SVN helper peptide for 6 h, and 10 μg/ml brefeldin A (Sigma–Aldrich) was added in the last 5 h. After cell surface and intracellular staining, IFN-γ production of CD4⁺ T cells was measured by FACS. Average percentages of IFN-γ-producing CD4⁺ T cells in response to (B) $OVA_{323-339}$ peptide; (C) Hs/Mm SVN_{53-67} peptide; (D) $MmSVN_{13-27}$ peptide; (E) $HsSVN_{13-27}$ peptide. *$p < 0.01$, **$p < 0.05$.

restimulated with $MmSVN_{13-27}$ or $HsSVN_{13-27}$ peptide (Fig. 4D, E). Differences in these two CD4 epitope sequences are in Fig. 2B.

Ab production by immunization with MmSVN2B with polyI:C

Activation of Th1 cells is essential for B cell antibody class switching. Therefore, we examined production of SVN-specific Ab in Tg mice that did or did not receive polyI:C. Serum was collected from HLA24^b-Tg mice immunized with different Ags and polyI:C. OVA and polyI:C were the positive control and resulted in a significant increase in OVA-specific IgG1, IgG2a and IgG2b by ELISA (Fig. 5 left panels). When HLA24^b-Tg mice were immunized with MmSVN2B or HsSVN2B without polyI:C, no significant production of any isotypes was observed (Fig. 5 center and right panels). When polyI:C was included, MmSVN2B or HsSVN2B-specific isotypes increased significantly.

Discussion

We demonstrated that HLA24^b-Tg mice induced $Hs/MmSVN_{53-67}$-specific CD4⁺ T cells and SVN-specific Ab followed by Th1 cell activation in response to injection of polyI:C and MmSVN2B protein. This result was partly inconsistent with a previous report (Charalambous et al. 2006) using Balb/c mice and HsSVN conjugated to Dec205 mAb. That is, our study with C57BL/6 mice and MmSVN2B did not detect significant increases in $MmSVN_{13-27}$-specific CD4⁺ T cells after subcutaneous injection of MmSVN2B with polyI:C. Thus, the xenogeneic differences in sequence between HsSVN and MmSVN did not always contribute to generating effective CD4⁺ T cells specific for a tumorigenic protein in C57BL/6 mice. The haplotype of the MHC class II proteins between Balb/c (having H-2d) and C57BL/6 mice (having H-2b) and Dec205 mAb conjugation (Charalambous et al. 2006) might be the reason for these different results. However, no CD8⁺ CTLs against the 2B peptide were detected even when using a specific tetramer for detection of CD8⁺ CTLs (Fig. S1). Hence, polyI:C was required for proliferation of self-reactive CD4⁺ Th1 cells that recognized the syngeneic epitope without proliferation of SVN2B peptide-specific CTLs.

OVA were used as positive controls (Fig. 3A, B left panels), and SL8 (SIINFEKL)-specific CTLs were monitored with OVA tetramer (Azuma et al. 2012). Here, T cell activation by polyI:C + MmSVN2B is a focus in this study. However, there is a lot-to-lot difference of T cell-activating activity in polyI:C + OVA as in our present and previous studies (Azuma et al. 2012). This difference of T cell activation may be attributable to the fact that polyI:C consists of a variety of length of polyI chains and polyC chains with a lot-to-lot heterogeneity. In addition, the amounts of Ags in Azuma's experiment are higher than those in the present experiment (Azuma et al. 2012). CD40 stimulation by specific Ab results in high enhancement of cross-priming of CD8 T cells (Charalambous et al. 2006) and CD40 was up-regulated in CD8α⁺ DCs by polyI:C treatment, but the CD40

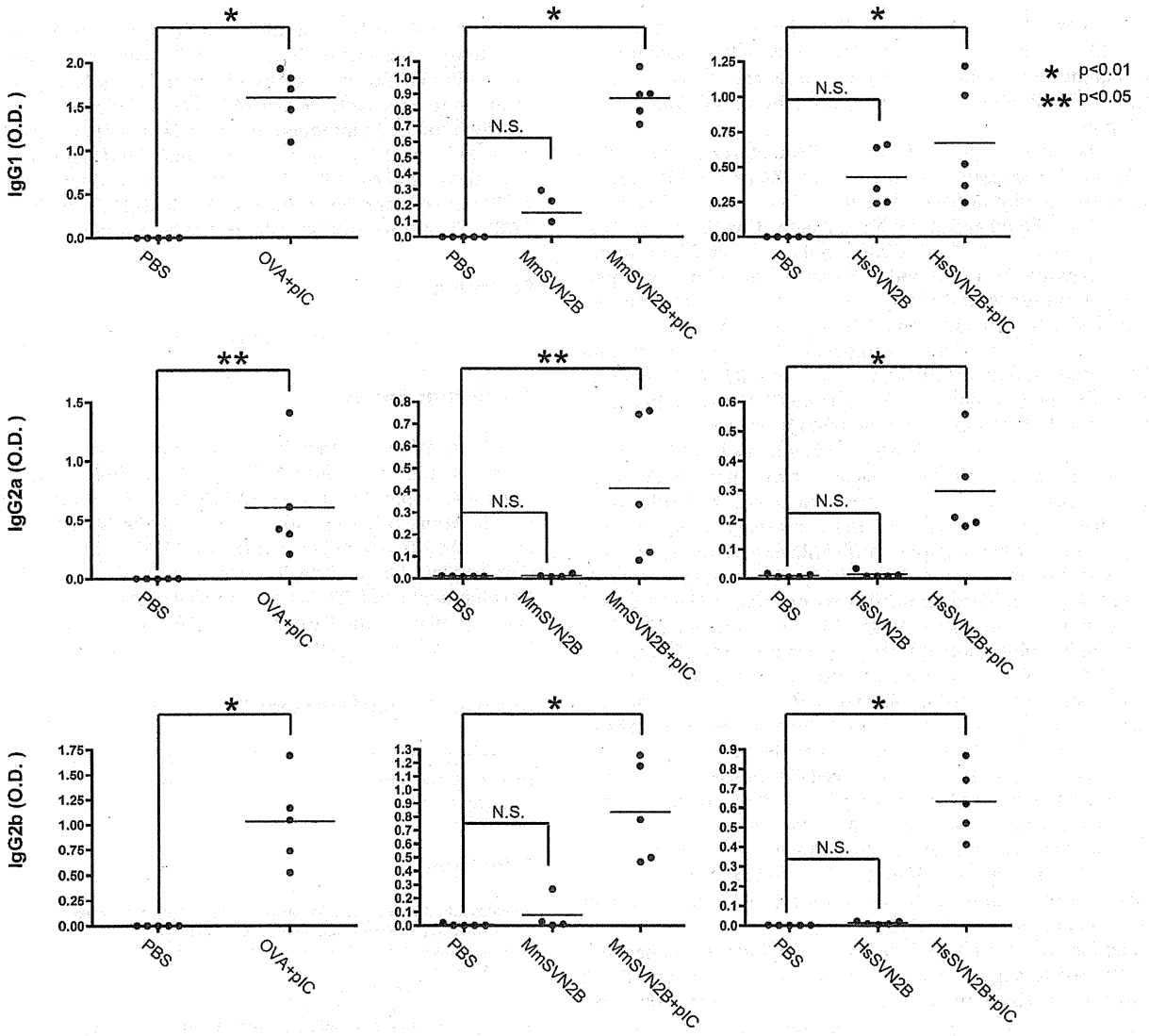

Fig. 5. Production of OVA and SVN-specific antibodies. Sera were collected from immunized mice at once a week for 4 weeks. Anti-OVA or anti-SVN in sera was assessed by ELISA using antiserum for IgG2a/b and IgG1. $^{*}p < 0.01$, $^{**}p < 0.05$.

levels were also variable depending upon the polyI:C lots. Development of a synthesizing method for defined length of RNA duplex will settle the issue.

Two points are noted. First, polyI:C, an RNA adjuvant, induces $CD4^+$ T cells in addition to the reported cases of $CD8^+$ T cells. The factors that participate in polyI:C-mediated CD4+ T cell proliferation and the kind of $CD4^+$ T subsets that are predominantly induced by polyI:C remain unknown. PolyI:C is primarily a potential activator of the IFN-inducing pathways RIG-I/MDA5 and TLR3 (Matsumoto & Seya 2008). These pathways allow host immune cells to produce type I/III IFNs and cytokines and are soluble effectors against cancer. TLR3 preferentially induces cross-presentation in $CD8\alpha^+$ DC in response to dsRNA including polyI:C (Schulz et al., 2005; Azuma et al. 2012) and causes proliferation of $CD8^+$ T cells including cells that respond to TAAs *via* cross-priming (Azuma et al. 2012). $CD4^+$ T cells that are likely evoked by polyI:C stimulation function in antitumor immunity since their helper function is usually suppressed in tumor-bearing mice and can be relieved by innate immune response (Lee et al. 2013). Stimulation with polyI:C + SVN Ag might change a tumor-derived suppressive environment to an environment suitable for primary activation and maintenance of Ag-specific cytotoxic $CD8^+$ T cell responses (Ridge et al. 1998; Janssen et al. 2003).

According to a recent report, however, adoptively transferred $CD4^+$ T cells induce tumor rejection independently of $CD8^+$ T cells (Corthay et al. 2005; Perez-Diez et al. 2007). This rejection is apparently based on cytokines released from $CD4^+$ T cells (Corthay et al. 2005) and on interaction with $CD4^+$ T cells and other immune cells such as macrophages (Mfs) and natural killer (NK) cells (Perez-Diez et al. 2007). DCs stimulated with polyI:C also result in NK cell activation after DC-NK cell-to-cell contact (Akazawa et al. 2007). Mfs in tumors might be a direct target of dsRNA, which converts tumor-supporting Mfs into tumoricidal Mfs (Shime et al. 2012). IL-12p40 is preferentially produced *via* the TICAM-1/Batf3 pathway in response to dsRNA (Azuma et al. 2013). Thus, a variety of cellular effectors can be triggered as antitumor agents by administration of dsRNA with TAA peptides or proteins. We found that $CD4^+$ T cells with Th1 properties were effectors induced by polyI:C possibly acting as an antitumor agent in SVN-responding tumor cells. Although epitope sequence and hydrophobicity might affect Th1 polarization in mice, $CD4^+$ T effectors are successfully induced in tumor-bearing or tumor-implanted mice by stimulation with MmSVN2B + polyI:C.

Hence, *in vivo* administration of an RNA adjuvant with Ag proteins induce $CD4^+$ helper T cells secondary to class II presentation in DCs, together with induction of type I IFNs and cytokines. $CD4^+$ T cells also facilitate Ab production caused by stimulation of B cell development (Mak et al. 2003).

Notably, this is a specific feature of RNA adjuvants, since TLR2 agonist Pam2 lipopeptides such as Pam2CSK4 and MALP2s induce antitumor CTLs with sufficient potential (Chua et al. 2014) but fail to induce DC-mediated antitumor NK cell activation (Yamazaki et al. 2011; Sawahata et al. 2011). $CD4^+$ T cells with regulatory modes such as Tregs and Tr-1 cells and IL-10 were induced by Pam2 peptide in the presence of Ag (Yamazaki et al. 2011). Nevertheless, robust proliferation of antitumor CTL is induced by Pam2 lipopeptides (Chua et al. 2014). Thus, the mode of $CD8^+$ T cell proliferation is differentially modulated between TLR2 and TLR3/MDA5 agonists.

The other point is how self-Ag-reactive $CD4^+$ T cells that act as Th1 effectors in SVN-based immunotherapy are generated. Proliferation of self-reactive T cells is prevented in normal mice, so the levels of self-reactive T cells are usually lower than the detection limit of assays (Gebe et al. 2003). Self-reactive $CD4^+$ T cells might be positively regulated by polyI:C in the presence of protein antigen, since mice, when exposed to DNA/RNA, harbor autoimmune diseases against the protein (Mills 2011). However, even with Ag proteins, polyI:C induced minimal cross-priming of $CD8^+$ T cells in our setting, as with previous reports (Charalambous et al. 2006). In this and other studies, both syngeneic and xenogeneic CD4 epitopes prime $CD4^+$ T cells, stimulating Ab production and Th1 polarization with antitumor activity, but with little association with CTL induction (Charalambous et al. 2006). Our SVN results suggested that self-responsive CD4 epitopes that are identical in sequence in human and mouse SVN have a conserved function as a Th1 skewer, albeit modest, in mice by stimulating DCs and Mfs to prime T and B cells. In this context, however, a question remains to be settled about why the insertion of the 2B sequence in MmSVN caused induction of auto-reactive $CD4^+$ T cells secondary to the class II presentation of the common SVN sequence (53-67) rather than the reported uncommon 13–27 region.

Generally, the presence of Tregs and regulatory cytokines such as IL-10 usually suppresses the function of self-reactive $CD4^+$ T effectors, so an autoimmune response cannot be detected (Danke et al. 2004; Quezada et al. 2010). In tumor-bearing mice, polyI:C releases the restriction of T cell autoreactivity by Tregs to enhance $CD4^+$ T function in a tumor microenvironment. Although the level of Treg cells increases in MALP2s-stimulated tumor-bearing mice (Yamazaki et al. 2011), the amount of Treg cells is not affected by polyI:C injection (Chua et al. 2014). Signs of autoimmune diseases have not yet been observed in mice that received intermittent administration of polyI:C under our conditions. Further studies on the function of regulatory factors in tumor-bearing mice after treatment with various adjuvants are needed to determine the balance between $CD4^+$ T effector functions and regulatory factors including Tregs (Quezada et al. 2010; Corthay et al. 2005).

It has been reported that treatment of murine glioma with DCs loading MmSVN long overlapping peptide covering CD4 and CD8 epitopes (DC therapy) conferred good prognosis on tumor-bearing mice (Ciesielski et al., 2008). In previous trials on peptide vaccine therapy, SVN2B peptide + IFN-α resulted in clinical improvements and enhanced immunological responses of patients (Kameshima et al. 2013). Treatment with SVN2B peptide alone did not result in good prognosis or effective tumor regression in late stage patients with cancer, however (Tsuruma et al. 2008; Honma et al. 2009). These results suggest that both killer and helper T cells are required for *in vivo* induction of tumor regression, as previously suggested (Perez-Diez et al. 2007). NK cells, Mfs, and soluble and angiogenetic factors might be involved in tumor rejection (Shime et al. 2012; Müller-Hermelink et al., 2008; Coussens and Werb 2002) in addition to Ag + polyI:C. According to the study with Ag and polyI:C, a protein or long peptide Ag containing CD4 epitopes, adjuvant RNA and additional factors that disable immunoregulatory factors, are required to effectively induce TAA-specific killer and helper T cell proliferation and subsequent tumoricidal activity in future studies (Casares et al. 2001). Ag peptides should be designed to present both class I and class II peptides on DCs to facilitate proliferation of $CD4^+$ T cells and Ab production. Methods for inducing potential $CD8^+$ CTLs against tumors still need to be considered.

Competing interests

The authors have declared that no competing interest exists.

Acknowledgements

We are grateful to members in our laboratories. JK is a Research Fellow of the Japan Society for the Promotion of Science. This work was supported in part by Grants-in-Aid from the Ministry of Education, Science, and Culture and the Ministry of Health, Labor, and Welfare of Japan, and by a MEXT Grant-in-Project 'the Carcinogenic Spiral', 'the National Cancer Center Research and Development Fund (23-A-44)'. Financial support by the Takeda Science Foundation, the Yasuda Cancer Research Foundation and the Ono Foundation are gratefully acknowledged.

Appendix A. Supplementary data

Supplementary data associated with this article can be found, in the online version, at http://dx.doi.org/10.1016/j.imbio.2014.08.017.

References

Ahonen, C.L., Doxsee, C.L., McGurran, S.M., Riter, T.R., Wade, W.F., Barth, R.J., Vasilakos, J.P., Noelle, R.J., Kedl, R.M., 2004. Combined TLR and CD40 triggering induces potent CD8+ T cell expansion with variable dependence on type I IFN. J. Exp. Med. 199, 775–784.

Altieri, D.C., 2001. The molecular basis and potential role of survivin in cancer diagnosis and therapy. Trends Mol. Med. 7, 542–547.

Akazawa, T., Ebihara, T., Okuno, M., Okuda, Y., Shingai, M., Tsujimura, K., Takahashi, T., Ikawa, M., Okabe, M., Inoue, N., Okamoto-Tanaka, M., Ishizaki, H., Miyoshi, J., Matsumoto, M., Seya, T., 2007. Antitumor NK activation induced by the Toll-like receptor 3-TICAM-1 (TRIF) pathway in myeloid dendritic cells. Proc. Natl. Acad. Sci. U. S. A. 104, 252–257.

Ambrosini, G., Adida, C., Altieri, D.C., 1997. A novel anti-apoptosis gene, survivin, expressed in cancer and lymphoma. Nat. Med. 3, 917–921.

Andersen, M.H., Pedersen, L.O., Becker, J.C., Straten, P.T., 2001. Identification of a cytotoxic T lymphocyte response to the apoptosis inhibitor protein survivin in cancer patients. Cancer Res. 61, 869–872.

Azuma, M., Ebihara, T., Oshiumi, H., Matsumoto, M., Seya, T., 2012. Cross-priming for antitumor CTL induced by soluble Ag + polyI:C depends on the TICAM-1 pathway in mouse CD11c(+)/CD8α(+) dendritic cells. Oncoimmunology 1, 581–592.

Azuma, M., Matsumoto, M., Seya, T., 2013. PolyI:C-derived dendritic cell maturation and cellular effectors depend on TICAM-1-Batf3 axis in mice. Proc. Jpn. Cancer Assoc. 72, 126.

Bevan, M.J., 1976. Cross-priming for a secondary cytotoxic response to minor H antigens with H-2 congenic cells which do not cross-react in the cytotoxic assay. J. Exp. Med. 143, 1283–1288.

Casares, N., Lasarte, J.J., de Cerio, A.L., Sarobe, P., Ruiz, M., Melero, I., Prieto, J., Borrás-Cuesta, F., 2001. Immunization with a tumor-associated CTL epitope plus a tumor-related or unrelated Th1 helper peptide elicits protective CTL immunity. Eur. J. Immunol. 31, 1780–1789.

Charalambous, A., Oks, M., Nchinda, G., Yamazaki, S., Steinman, R.M., 2006. Dendritic cell targeting of survivin protein in a xenogeneic form elicits strong CD4+ T cell immunity to mouse survivin. J. Immunol. 177, 8410–8421, 44.

Chua, B.Y., Olson, M.R., Bedoui, S., Sekiya, T., Wong, C.Y., Turner, S.J., Jackson, D.C., 2014. The use of a TLR2 agonist-based adjuvant for enhancing effector and memory CD8 T-cell responses. Immunol. Cell Biol., http://dx.doi.org/10.1038/icb.2013.102.

Ciesielski, M.J., Kozbor, D., Castanaro, C.A., Barone, T.A., Fenstermaker, R.A., 2008. Therapeutic effect of a T helper cell supported CTL response induced by a survivin peptide vaccine against murine cerebral glioma. Cancer Immunol. Immunother. 57, 1827–1835.

Corthay, A., Skovseth, D.K., Lundin, K.U., Rosjo, E., Omholt, H., Hofgaad, P.O., Haraldsen, G., Bogen, B., 2005. Primary antitumor immune response mediated by CD4+ T cells. Immunity 22, 371–383.
Coussens, L.M., Werb, Z., 2002. Inflammation and cancer. Nature 420, 860–867.
Danke, N.A., Koelle, D.M., Yee, C., Beheray, S., Kwok, W.W., 2004. Autoreactive T cells in healthy individuals. J. Immunol. 172, 5967–6572.
Fukuda, S., Pelus, L.M., 2006. Survivin, a cancer target with an emerging role in normal adult tissues. Mol. Cancer Ther. 5, 1087–1098.
Gebe, J.A., Falk, B.A., Rock, K.A., Kochik, S.A., Heninger, A.K., Reijonen, H., Kwok, W.W., Nepom, G.T., 2003. Low-avidity recognition by CD4+ T cells directed to self-antigens. Eur. J. Immunol. 33, 1409–1417.
Gotoh, M., Takasu, H., Harada, K., Yamaoka, T., 2002. Development of HLA-A2402/K^b transgenic mice. Int. J. Cancer 100, 565–570.
Hirohashi, Y., Torigoe, T., Maeda, A., Nabeta, Y., Kamiguchi, K., Sato, T., Yoda, J., Ikeda, H., Hirata, K., Yamanaka, N., Sato, N., 2002. An HLA-A24-restricted cytotoxic T lymphocyte epitope of a tumor-associated protein, survivin. Clin. Cancer Res. 8, 1731–1739.
Honma, I., Kitamura, H., Torigoe, T., Takahashi, A., Tanaka, T., Sato, E., Hirohashi, Y., Masumori, N., Tsukamoto, T., Sato, N., 2009. Phase I clinical study of anti-apoptosis protein survivin-derived peptide vaccination for patients with advanced or recurrent urothelial cancer. Cancer Immunol. Immunother. 58, 1801–1807.
Idenoue, S., Hirohashi, Y., Torigoe, T., Sato, Y., Tamura, Y., Hariu, H., Yamamoto, M., Kurotaki, T., Tsuruma, T., Asanuma, H., Kanaseki, T., Ikeda, H., Kashiwagi, K., Okazaki, M., Sasaki, K., Sato, T., Ohmura, T., Hata, F., Yamaguchi, K., Hirata, K., Sato, N., 2005. A potent immunogenic general cancer vaccine that targets survivin, an inhibitor of apoptosis proteins. Clin. Cancer Res. 11, 1474–1482.
Janssen, E.M., Lemmens, E.E., Wolfe, T., Christen, U., von Herrath, M.G., et al., 2003. CD4+ T cells are required for secondary expansion and memory in CD8+ T lymphocytes. Nature 421, 852–856.
Kameshima, H., Tsuruma, T., Kutomi, G., Shima, H., Iwayama, Y., Kimura, Y., Imamura, M., Torigoe, T., Takahashi, A., Hirohashi, Y., Tamura, Y., Tsukahara, T., Kanaseki, T., Sato, N., Hirata, K., 2013. Immunotherapeutic benefit of α-interferon (IFNα) in survivin2B-derived peptide vaccination for advanced pancreatic cancer patients. Cancer Sci. 104, 124–129.
Kobayashi, K., Hatano, M., Otaki, M., Ogasawara, T., Tokuhisa, T., 1999. Expression of a murine homologue of the inhibitor of apoptosis protein is related to cell proliferation. Proc. Natl. Acad. Sci. U. S. A. 96, 1457–1462.
Lee, M.K.4th, Xu, S., Fitzpatrick, E.H., Sharma, A., Graves, H.L., Czerniecki, B.J., 2013. Inhibition of CD4+CD25+ regulatory T cell function and conversion into Th1-like effectors by a Toll-like receptor-activated dendritic cell vaccine. PLOS ONE 8, e74698.
Li, F., 2005. Role of survivin and its splice variants in tumorigenesis. Br. J. Cancer 92, 212–216.
Mahotka, C., Wenzel, M., Springer, E., Gabbert, H.E., Gerharz, C.D., 1999. Survivin-deltaEx3 and survivin-2B: two novel splice variants of the apoptosis inhibitor survivin with different antiapoptotic properties. Cancer Res. 59, 6097–6102.
Mahotka, C., Liebmann, J., Wenzel, M., Suschek, C.V., Schmitt, M., Gabbert, H.E., Gerharz, C.D., 2002. Differential subcellular localization of functionally divergent surviving splice variants. Cell Death Differ. 9, 1334–1342.
Mak, T.W., Shahinian, A., Yoshinaga, S.K., Wakeham, A., Boucher, L.M., Pintilie, M., Duncan, G., Gajewska, B.U., Gronski, M., Eriksson, U., Odermatt, B., Ho, A., Bouchard, D., Whorisky, J.S., Jordana, M., Ohashi, P.S., Pawson, T., Bladt, F., Tafuri, A., 2003. Costimulation through the inducible costimulator ligand is essential for both T helper and B cell functions in T cell-dependent B cell responses. Nat. Immunol. 4, 765–772.
Matsumoto, M., Seya, T., 2008. TLR3: interferon induction by double-stranded RNA including poly(I:C). Adv. Drug Deliv. Rev. 60, 805–812.
Mills, K.H., 2011. TLR-dependent T cell activation in autoimmunity. Nat. Rev. Immunol. 11, 807–822.
Müller-Hermelink, N., Braumüller, H., Pichler, B., Wieder, T., Mailhammer, R., Schaak, K., Ghoreschi, K., Yazdi, A., Haubner, R., Sander, C.A., Mocikat, R., Schwaiger, M., Förster, I., Huss, R., Weber, W.A., Kneilling, M., Röcken, M., 2008. TNFR1 signaling and IFN-gamma signaling determine whether T cells induce tumor dormancy or promote multistage carcinogenesis. Cancer Cell 13, 507–518.
Nishiguchi, M., Matsumoto, M., Takao, T., Hoshino, M., Shimonishi, Y., Tsuji, S., Begum, N.A., Takeuchi, O., Akira, S., Toyoshima, K., Seya, T., 2001. Mycoplasma *fermentans* lipoprotein M161Ag-induced cell activation is mediated by Toll-like receptor 2: role of N-terminal hydrophobic portion in its multiple functions. J. Immunol. 166, 2610–2616.
Okada, H., Bakal, C., Shahinian, A., Elia, A., Wakeham, A., Suh, W.K., Duncan, G.S., Ciofani, M., Rottapel, R., Zuniga-Pflucker, J.C., Mak, T.W., 2004. Survivin loss in thymocytes triggers p53-mediated growth arrest and p53-independent cell death. J. Exp. Med. 199, 399–410.
Osen, W., Soltek, S., Song, M., Leuchs, B., Steitz, J., Tüting, T., Eichmüller, S.B., Nguyen, X.D., Schadendorf, D., Paschen, A., 2010. Screening of human tumor antigens for CD4 T cell epitopes by combination of HLA-transgenic mice, recombinant adenovirus and antigen peptide libraries. PLOS ONE 5, e14137.
Perez-Diez, A., Joncker, N.T., Choi, K., Chan, W.F., Anderson, C.C., Lantz, O., Matzinger, P., 2007. CD4 cells can be more efficient at tumor rejection than CD8 cells. Blood 109, 5346–5354.
Quezada, S.A., Simpson, T.R., Peggs, K.S., Merghoub, T., Vider, J., Fan, X., Blasberg, R., Yagita, H., Muranski, P., Antony, P.A., Restifo, N.P., Allison, J.P., 2010. Tumor-reactive CD4(+) T cells develop cytotoxic activity and eradicate large established melanoma after transfer into lymphopenic hosts. J. Exp. Med. 207, 637–650.
Ridge, J.P., Di Rosa, F., Matzinger, P., 1998. A conditioned dendritic cell can be a temporal bridge between a CD4+ T-helper and a T-killer cell. Nature 393, 474–478.
Rosenberg, S.A., Yang, J.C., Restifo, N.P., 2004. Cancer immunotherapy: moving beyond current vaccines. Nat. Med. 10, 909–915.
Sawahata, R., Shime, H., Yamazaki, S., Inoue, N., Akazawa, T., Fujimoto, Y., Fukase, K., Matsumoto, M., Seya, T., 2011. Failure of mycoplasma lipoprotein MALP-2 to induce NK cell activation through dendritic cell TLR2. Microbes Infect. 13, 350–358.
Schmitz, M., Diestelkoetter, P., Weigle, B., Schmachtenberg, F., Stevanovic, S., Ockert, D., Rammensee, H.G., Rieber, E.P., 2000. Generation of survivin-specific CD8+ T effector cells by dendritic cells pulsed with protein or selected peptides. Cancer Res. 60, 4845–4849.
Schulz, O., Diebold, S.S., Chen, M., Näslund, T.I., Nolte, M.A., Alexopoulou, L., Azuma, Y.T., Flavell, R.A., Liljeström, P., Reis e Sousa, C., 2005. Toll-like receptor 3 promotes cross-priming to virus-infected cells. Nature 433, 887–892.
Seya, T., Matsumoto, M., 2009. The extrinsic RNA-sensing pathway for adjuvant immunotherapy of cancer. Cancer Immunol. Immunother. 58, 1175–1184.
Seya, T., Azuma, M., Matsumoto, M., 2013. Targeting TLR3 with no RIG-I/MDA5 activation is effective in immunotherapy for cancer. Expert Opin. Ther. Targets 17, 533–544.
Shime, H., Matsumoto, M., Oshiumi, H., Tanaka, S., Nakane, A., Iwakura, Y., Tahara, H., Inoue, N., Seya, T., 2012. Toll-like receptor 3 signaling converts tumor-supporting myeloid cells to tumoricidal effectors. Proc. Natl. Acad. Sci. U. S. A. 109, 2066–2071.
Topalian, S.L., Gonzales, M.I., Parkhurst, M., Li, Y.F., Southwood, S., Sette, A., Rosenberg, S.A., Robbins, P.F., 1996. Melanoma-specific CD4+ T cells recognize nonmutated HLA-DR-restricted tyrosinase epitopes. J. Exp. Med. 183, 1965–1971.
Tsuruma, T., Iwayama, Y., Ohmura, T., Katsuramaki, T., Hata, F., Furuhata, T., Yamaguchi, K., Kimura, Y., Torigoe, T., Toyota, N., Yagihashi, A., Hirohashi, Y., Asanuma, H., Shimozawa, K., Okazaki, M., Mizushima, Y., Nomura, N., Sato, N., Hirata, K., 2008. Clinical and immunological evaluation of anti-apoptosis protein, survivin-derived peptide vaccine in phase I clinical study for patients with advanced or recurrent breast cancer. J. Transl. Med. 6, 24.
Yamazaki, S., Okada, K., Maruyama, A., Matsumoto, M., Yagita, H., Seya, T., 2011. TLR2-dependent induction of IL-10 and Foxp3+ CD25+ CD4+ regulatory T cells prevents effective anti-tumor immunity induced by Pam2 lipopeptides in vivo. PLOS ONE 6, e18833.

nature COMMUNICATIONS

ARTICLE

Received 7 Nov 2014 | Accepted 13 Jan 2015 | Published 18 Feb 2015

DOI: 10.1038/ncomms7280

Defined TLR3-specific adjuvant that induces NK and CTL activation without significant cytokine production *in vivo*

Misako Matsumoto[1], Megumi Tatematsu[1], Fumiko Nishikawa[1], Masahiro Azuma[1,†], Noriko Ishii[1], Akiko Morii-Sakai[1], Hiroaki Shime[1] & Tsukasa Seya[1]

Ligand stimulation of the Toll-like receptors (TLRs) triggers innate immune response, cytokine production and cellular immune activation in dendritic cells. However, most TLR ligands are microbial constituents, which cause inflammation and toxicity. Toxic response could be reduced for secure immunotherapy through the use of chemically synthesized ligands with defined functions. Here we create an RNA ligand for TLR3 with no ability to activate the RIG-I/MDA5 pathway. This TLR3 ligand is a chimeric molecule consisting of phosphorothioate ODN-guided dsRNA (sODN-dsRNA), which elicits far less cytokine production than poly(I:C) *in vitro* and *in vivo*. The activation of TLR3/TICAM-1 pathway by sODN-dsRNA effectively induces natural killer and cytotoxic T cells in tumour-loaded mice, thereby establishing antitumour immunity. Systemic cytokinemia does not occur following subcutaneous or even intraperitoneal administration of sODN-dsRNA, indicating that TICAM-1 signalling with minute local cytokines sufficiently activate dendritic cells to prime tumoricidal effectors *in vivo*.

[1] Department of Microbiology and Immunology, Hokkaido University Graduate School of Medicine, Kita 15, Nishi 7, Kita-ku, Sapporo 060-8638, Japan. † Present address: Department of Pathology and Cellular Biology, University of Montreal, 2900 Edouard-Montpetit, Montreal, Quebec, Canada H3T 1J4. Correspondence and requests for materials should be addressed to M.M. (email: matumoto@pop.med.hokudai.ac.jp) or to T.S. (email: seya-tu@pop.med.hokudai.ac.jp).

Double-stranded (ds) RNA is often a signature of viral infection, which induces production of type I interferon (IFN) and inflammatory cytokines[1,2]. Its putative analogue polyinosinic:polycytidylic acid (poly(I:C)) exhibits both strong antiviral and anticancer potential[3,4]. Poly(I:C) has been considered a promising adjuvant for cancer immunotherapy for several decades[4–6]. In mouse models, growth retardation of syngenic implant tumours is observed following administration of poly(I:C)[7,8], which is due to dendritic cell (DC)-derived natural killer (NK) and cytotoxic T-cell (CTL) activity[9,10]. Nevertheless, it has not been successfully used therapeutically in patients with cancer[5,6]. The amount of poly(I:C) required for an adequate therapeutic response causes side effects, including arthlargia, fever, erythema and sometimes life-threatening endotoxin-like shock[5,6], which have prevented application of this dsRNA analogue from the clinical use. These side effects may be related to cytokine storm induced by dsRNA, although the situation is somewhat alleviated when minimal poly(I:C)-LC (poly-L-lysine and methylcellulose) is used instead of effector-inducible doses of mere poly(I:C) alone[5,6,11].

According to recent understanding on pattern recognition of innate immunity, poly(I:C) is a ligand for multiple pattern recognition receptors (PRRs), including protein kinase R, retinoic acid-inducible gene-I (RIG-I), melanoma differentiation-associated gene 5 (MDA5) and Toll-like receptor (TLR) 3 (refs 1,4,12). Virus replication usually produces dsRNA within the cytoplasm of infected cells and stimulates the cytoplasmic RNA sensors[12,13]. In contrast, TLR3 is activated when dsRNA liberated from virus-infected cells is internalized into the endosome of non-infected phagocytes[4,14], such as DCs and macrophages. Type I IFN and DC-mediated immune responses are evoked to suppress virus replication. Physiologically, these responses occur in a complex manner, therefore, what happens *in vivo* when only a single receptor is stimulated remains to be elucidated, whereas what happens *in vivo* when a single gene is disrupted has been reported in knockout (KO) mouse studies[1]. It is therefore crucial in drug design to create PRR ligands specific for each PRR for the development of immune adjuvant.

Regression of tumour with a lesser major histocompatibility complex expression[15] is caused by reciprocal activation of NK cells by poly(I:C)-stimulated DC[9,16]. However, in antitumour immunity, constitutive proliferation of antitumour CTL is important and antigen (Ag)-presenting DC must capture not only innate patterns but also tumour-associated Ag (TAA) for their cross-priming[10,17]. $CD8\alpha^+$ DC in mouse lymphoid tissue[10,18,19] and $CD103^+$ and $CD141^+$ DCs in humans[18–20] are representative subsets that express TLR3 and induce efficient Ag cross-presentation in response to dsRNA enabling presentation of Ags to $CD8^+$ T cells on their major histocompatibility complex class I proteins. In contrast, interleukin (IL)-12, IL-6, tumour necrosis factor (TNF)-α and IFN-α/β are the main mediators released in the serum secondary to exogenously administered poly(I:C)[4,20,21]. Studies in KO mice suggested that TLR3 has a pivotal role in inducing cross-presentation[10,17], but its role is marginal in systemic cytokine/IFN production *in vivo*[21]. Most cytokines (except IL-12 p40) and type I IFN detected in serum are attributable to poly(I:C)'s stimulation of RIG-I and/or MDA5, that is, the mitochondrial antiviral-signalling protein (MAVS) pathway[12,21]. CTL/NK cell activation and robust cytokine production can be assigned, although partly overlapping, to the TLR3/Toll-IL-1 receptor domain-containing adaptor molecule (TICAM)-1 or MAVS pathway, respectively.

Here we generated synthetic dsRNA derivatives expected to specifically act on TLR3, but not on RIG-I/MDA5. These ligands exhibited strong activity in inducing antitumour CTL and NK cells and caused marked regression of tumours without off-target effects including significant increases of serum cytokine/IFN levels in mouse models.

Results

Design of novel TLR3 agonist. What we experienced in developing an RNA adjuvant was that: very little *in vitro* transcribed dsRNAs entered the human cells[22], whereas poly(I:C) as well as CpG or control GpC phosphorothioate oligodeoxynucleotides (sODNs) reached the endosome in human myeloid DCs and epithelial cells. Poly(I:C) and sODNs appeared to share the uptake receptor[23]. To deliver dsRNA to endosome TLR3, we have connected sODN to 5′ sense RNA and annealed it with antisense RNA (Fig. 1a) to guide dsRNA internalization into TLR3-positive endosomes. The RNA source was chosen from a vaccine strain of measles virus (MV), as children around the world undergo MV vaccination without severe adverse events. Because >40 bp dsRNA may be the minimal length for activation of TLR3 (ref. 24), we selected the region of defective interference RNA in the vaccine MV that causes no RNA interference[25].

Because direct chemical synthesis of long sequences of RNA was unfeasible in our laboratory until recently, we first made the RNA duplex structures by *in vitro* transcription and annealing. sODN was connected via a linker DNA to dsRNA, so the three-chain structures were first designed (Fig. 1b) to carry forward by many trial-and-error tests for a specific TLR3 agonist. A GpC-type sODN cap cM362 (Fig. 1a,b) facilitates targeting to TLR3-positive endosomes, does not activate TLR9 and blocks dsRNA-mediated RIG-I/MDA5 activation; therefore it meets our criteria for a single PRR agonist.

Testing function of *in vitro* transcribed sODN-dsRNAs. Various kinds of sODN-dsRNA hybrid molecules were prepared by *in vitro* transcription and annealing (Supplementary Fig. 1a, Supplementary Tables 1 and 2). In preliminary experiments to screen for a preferential sODN-dsRNA, we tested reporter gene (Luc125 for IFN-β promoter) activation in HEK293 cells expressing human TLR3.

sODN-dsRNAs with dsRNA of >99 bp in length induced TLR3-dependent IFN-β-promoter activation similar to that induced by poly(I:C) in the presence or absence of fetal calf serum (FCS), whereas sODN-dsRNAs with dsRNA of <79 bp induced hardly any activation of TLR3 (Supplementary Fig. 1b,c). Notably, none of the sODN-dsRNAs examined were able to activate cytoplasmic RNA sensors when transfected into HEK293 cells (Supplementary Fig. 2). We examined whether GpC motif or the length of sODN influenced the uptake of sODN-dsRNA. TLR3-mediated IFN-β promoter activation by sODN-dsRNA was independent of the presence of a GpC motif of sODN but dependent on the length; almost >20-mer of sODN is required for full activation of endosomal TLR3 (Supplementary Fig. 3). 139 bp dsRNA and control B-type (c2006) or C-type (cM362) sODN were good candidates for activation of endosomal TLR3 with no TLR9 activation.

We next examined the internalization of Cy3-labelled cM362-dsRNA (cM362-79, cM362-99 and cM362-139) in HeLa cells. cM362-dsRNAs were all similarly bound to the cell surface at 4 °C, but dsRNA73 and dsRNA139 without cM362 could not bind (Supplementary Fig. 4). When cells were incubated at 37 °C, cM362-99 and cM362-139 both entered the cells more quickly than cM362 and cM362-79, localized in the early endosome after 15 min incubation and were retained for up to 120 min, whereas cM362 and cM362-79 co-localized with EEA1 at a later time point (30 min) and quickly moved to the lysosomes. Localization of cM362-139 in the lysosomes was observed after 60 min

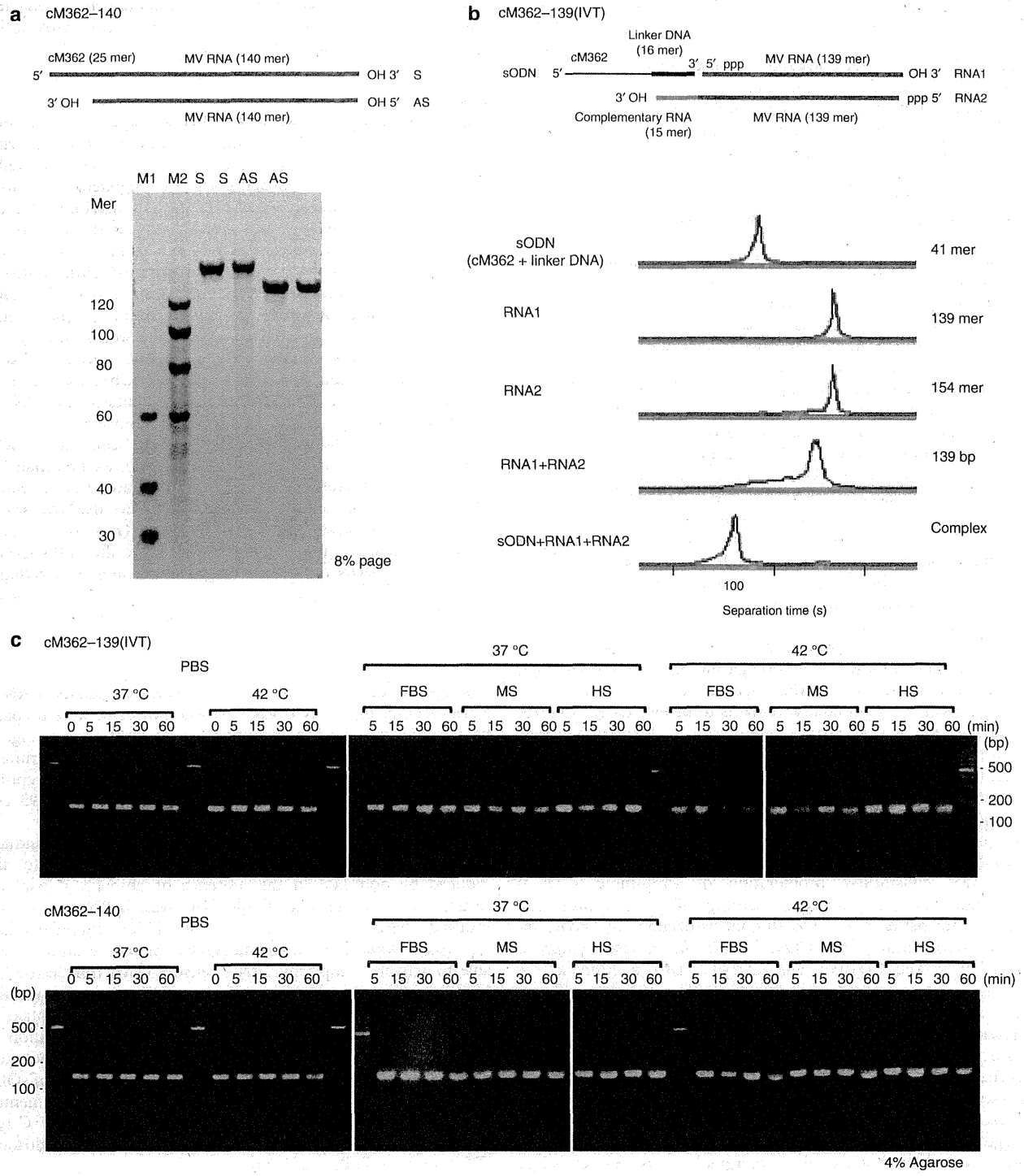

Figure 1 | Preparation of cM362-139 and cM362-140. (**a**) Schematic diagram of cM362-140. cM362-140 consists of chemically synthesized two nucleotide strands. The sense strand (S) is a 140 mer RNA capped with cM362 (25 mer) at 5′ site. The antisense strand (AS) is the complementary 140 mer RNA. Five pmol of S and AS RNAs were analysed on 8% PAGE containing 7M urea. M1 and M2, RNA size markers. (**b**) Schematic diagram of cM362-139(IVT) and its electropherograms. cM362-139(IVT) consists of three nucleotide strands, sODN (cM362 + linker DNA; 41 mer), *in vitro* transcribed sense RNA strand (RNA1; 139 mer) and antisense RNA strand (RNA2; 154 mer). All sequences of DNA and RNAs are described in Supplementary Tables. sODN, RNA1, RNA2, dsRNA (RNA1 + RNA2) and complex cM362-139 (sODN + RNA1 + RNA2) were analysed using multi-channel microchip electrophoresis. (**c**) Stability of cM362-139(IVT) and cM362-140. cM362-139(IVT) and cM362-140 were incubated in PBS with or without 10% heat-inactivated FBS, mouse serum (MS) or human serum (HS) at 37 °C or 42 °C for indicated time points. Aliquots containing 0.1 μg of treated cM362-dsRNAs were loaded onto a 4% agarose gel.